Mathematics and Computers in Simulation 234 (2025) 368–389

Contents lists available at ScienceDirect

Mathematics and Computers in Simulation

journal homepage: www.elsevier.com/locate/matcom

Original articles

A family of C^1 Clough–Tocher spline spaces on C^0 piecewise quadratic domain partitions

Jan Grošelj, Marjeta Knez *

Faculty of Mathematics and Physics, University of Ljubljana, Jadranska 19, 1000 Ljubljana, Slovenia
Institute of Mathematics, Physics and Mechanics, Jadranska 19, 1000 Ljubljana, Slovenia

ARTICLE INFO

Keywords:
Quadratic triangle
Quadratic triangulation
Isogeometric functions
Clough–Tocher refinement
Spline space
Dimension
Basis functions

ABSTRACT

The paper addresses the construction of C^1 splines on a curved domain that is parametrized by a C^0 piecewise geometry mapping composed of quadratic Bézier triangles. The C^1 splines are assembled from polynomials of a chosen total degree greater than or equal to four, and their construction is based on the Clough–Tocher splitting technique that ensures locality. In particular, the splines are locally characterized by an interpolation problem described by Hermite data, which resembles the standard macro-element concepts developed for C^1 splines on triangulations.

1. Introduction

Piecewise polynomial functions in two variables, commonly addressed as bivariate splines, are an indispensable tool in numerical approximation and modeling. When smoothness of order one or more is required, the splines most often in use are tensor product B-splines [1]. These splines are defined on a rectangular domain that is partitioned by a regular mesh induced by knot sequences of the underlying univariate B-splines in two directions. For more general domains and unstructured partitions, which frequently arise in practice, the theory of smooth bivariate splines is considerably more complicated and still an area of very active research.

One of the traditional unstructured spline technologies emerging from the classical finite element analysis are splines on a planar triangulation, *i.e.*, splines defined on a polygonal domain partitioned by a set of triangles. In this context, a spline restricted to a triangle is considered to be a bivariate polynomial of some fixed total degree, as opposed to a tensor product spline whose restriction to a local mesh element is a tensor product polynomial. The characterization of C^1 splines and splines of higher smoothness on a triangulation has proved to be incredibly challenging for low degrees with respect to the smoothness order [2]. Consequently, in practice, carefully tailored macro-element constructions are used, which typically determine a smooth spline by interpolation on each triangle separately and independently.

A common macro-element approach is to refine each triangle into three smaller triangles by introducing a split point inside the triangle. The Clough–Tocher splines, *i.e.*, C^1 cubic splines on the induced refinement, are characterized by interpolation of value and gradient at each vertex of the initial triangulation and interpolation of a directional derivative at a point inside of each edge of the initial triangulation [3]. This popular construction still remains a subject of modification and reinterpretation; see, *e.g.*, [4–6]. Recently, also a family of C^1 spline spaces of arbitrary degree greater than three on such a refinement has been introduced in [7].

For approximation of functions on a curved domain, one can resort to the isoparametric method, a well-established technique in the finite element analysis; see, *e.g.*, [8]. Its main idea is to consider a spline space $\mathbb{S}$ as the space spanned by functions on a parametric domain. Using these functions, one first parametrizes the curved domain by a diffeomorphic geometry mapping $\boldsymbol{F} \in \mathbb{S}\times\mathbb{S}$

* Corresponding author at: Faculty of Mathematics and Physics, University of Ljubljana, Jadranska 19, 1000 Ljubljana, Slovenia.
E-mail addresses: jan.groselj@fmf.uni-lj.si (J. Grošelj), marjetka.knez@fmf.uni-lj.si (M. Knez).

https://doi.org/10.1016/j.matcom.2025.03.006
Received 6 September 2024; Received in revised form 15 January 2025; Accepted 8 March 2025
Available online 19 March 2025

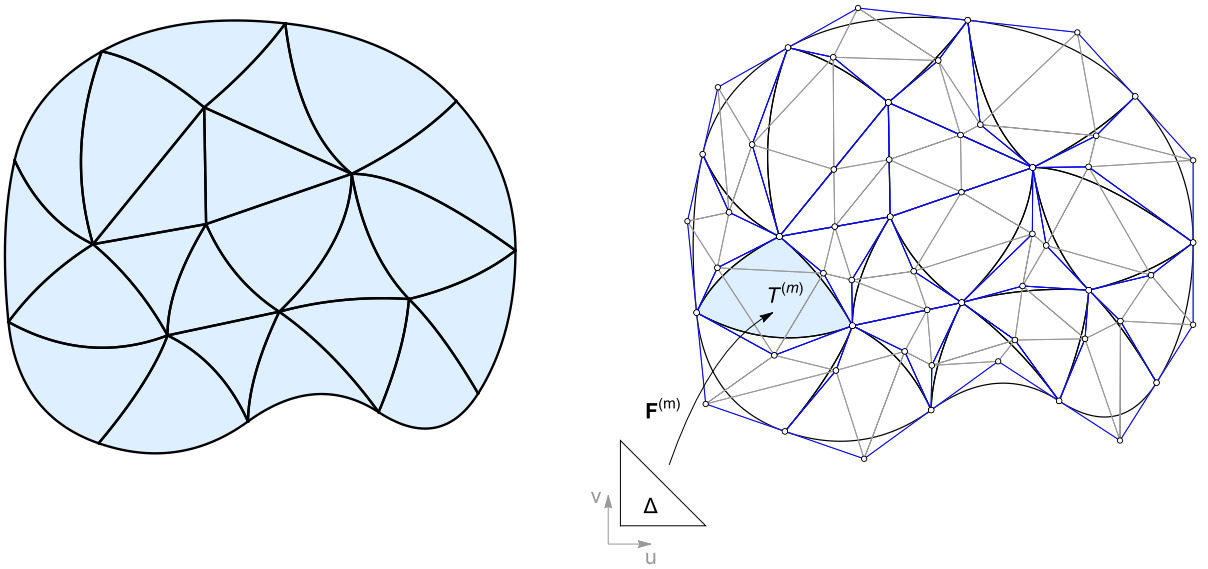

Fig. 1. An example of a planar domain composed of quadratic Bézier triangles, each of which is parametrized on the same unit triangle (as shown in the right picture).

and then seeks a solution φ to the approximation problem over the curved domain in the form of a spline $s \in \mathbb{S}$ on the parametric domain composed with the inverse of the geometry mapping, *i.e.*, $\varphi = s \circ \boldsymbol{F}^{-1}$. Thus φ is completely specified by $(\boldsymbol{F}, s) \in \mathbb{S} \times \mathbb{S} \times \mathbb{S}$ and both the geometry mapping $\boldsymbol{F}$ and the approximate solution s on the parametric domain are expressed by the same set of basis functions.

The concept of the isoparametric method has been highly popularized by the isogeometric analysis [9], which is a spin-off of the finite element analysis. The method utilizes tensor product B-splines for the basis functions on the parametric domain and provides a means of bridging the common discrepancy between the representation of objects in computer design and analysis. More recently, the ideas of isogeometric analysis have been considered in the context of macro-elements for unstructured domain partitions, including triangulations [10–12]. One particularly promising approach is the use of the C^1 Powell–Sabin splines [13], which can be represented by B-spline-like functions [14]. In this setting $s = \varphi \circ \boldsymbol{F}$ is a C^1 piecewise quadratic function and allows approximation of optimal (cubic) order [15]. A C^1 mapping $\boldsymbol{F}$ for a given domain boundary can be obtained by solving a suitable optimization problem [16].

In this paper, we pose a theoretically more challenging problem of constructing a C^1 function φ on a curved domain that is parametrized by only a C^0 piecewise quadratic geometry mapping $\boldsymbol{F}$, *i.e.*, a mapping $\boldsymbol{F}$ that in general cannot be globally represented as a linear combination of C^1 basis functions. Compared to the C^1 isoparametric mapping, such $\boldsymbol{F}$ is much easier to obtain and allows intuitive modeling of the domain, *e.g.*, one can start with a triangulation and use the extra control point of freedom associated with an edge in order to curve the edge into a parabola represented by a quadratic Bézier curve with the end control points located at the vertices of the triangulation (see Fig. 1 for an illustration). As shown in Fig. 1 (right) every quadratic Bézier triangle is parameterized with its own geometry mapping. Clearly, these mappings could be presented as a global bijective C^0 continuous quadratic spline mapping $\boldsymbol{F}$ from the domain (with piecewise linear boundary), partitioned by the corresponding triangulation, to the curved domain. Given such a curved domain and its induced partition into quadratic Bézier triangles, we consider the construction of C^1 splines on the domain by applying the Clough–Tocher splitting to the parametric domain of each Bézier triangle. We require that $s = \varphi \circ \boldsymbol{F}$ is a piecewise polynomial function of some fixed total degree $d \in \mathbb{N}$ and that φ is C^1 continuous.

Not surprisingly, the construction of φ in this context is more complicated than the construction of isoparametric splines. However, we show that for $d \geq 4$ the function φ can be constructed locally in a similar manner as the C^1 cubic and higher degree Clough–Tocher splines on a triangulation (see [7]). Using the theoretical results of [17], we provide a procedure to define such a spline via interpolation by specifying three degrees of freedom per vertex and additional degrees of freedom associated with triangles and edges of the triangulation. Per triangle, there are $\binom{d-2}{2}$ degrees of freedom, whereas the number of degrees of freedom associated with an edge is at least $2d - 7$ and varies depending on the parametrization of the quadratic Bézier triangles attached to the edge. These insights allow the construction of basis functions and the derivation of a bivariate interpolation method. In relation to the latter, the numerical results reported in this paper indicate that the proposed spline construction for degree d may allow the approximation of order d, which is only one less than optimal.

The remainder of the paper is organized as follows. In Section 2 we introduce the notion of a quadratic triangulation and define a spline space on such a partition. We also present C^1 smoothness conditions that are crucial for identifying degrees of freedom of the considered splines. Section 3 is devoted to the construction of C^1 smooth splines on a Clough–Tocher refined quadratic triangulation and their characterization in terms on an interpolation problem. A set of basis functions is proposed and some numerical examples of interpolation are provided. The paper concludes with a few remarks in Section 4.

2. Splines on a quadratic triangulation

In this section we first define a particular partition of a curved domain that we address as a quadratic triangulation and which is a generalization of the standard (linear) triangulation that comprises triangles covering a domain with a polygonal boundary. We then consider a general spline space over a quadratic triangulation and review the Bernstein–Bézier tools that are convenient for its analysis. Finally, we discuss C^1 smoothness conditions, the understanding of which is a crucial step to construct C^1 splines in the context of quadratic triangulations.

2.1. Quadratic triangulations

Let us start by introducing a quadratic triangle as the codomain of a quadratic polynomial mapping defined on

$$\triangle = \left\{(u,v) \in \mathbb{R}^2 \,:\; u \in [0,1],\; 0 \le v \le 1-u\right\}.$$

For a given degree $d \in \mathbb{N}_0$, we denote by $\mathbb{P}^2_d$ the space of bivariate polynomials of total degree at most d.

Definition 1 (*Quadratic Triangle*)**.** Let $\boldsymbol{F} \in \mathbb{P}^2_2 \times \mathbb{P}^2_2$ be a mapping that is injective on $\triangle$ and regular on $\triangle$ (*i.e.*, for every $(u,v) \in \triangle$, the determinant of the Jacobian matrix $J\boldsymbol{F}(u,v)$ is non-zero). Then, $[\boldsymbol{F}] := \boldsymbol{F}(\triangle)$ is a quadratic triangle and $\boldsymbol{F}$ its parametrization.

For notational convenience, we decompose the boundary of a quadratic triangle $T = [\boldsymbol{F}]$ into three vertices, *i.e.*,

$$\boldsymbol{V}_1 = [\boldsymbol{F}]_1 = \boldsymbol{F}(1,0), \quad \boldsymbol{V}_2 = [\boldsymbol{F}]_2 = \boldsymbol{F}(0,1), \quad \boldsymbol{V}_3 = [\boldsymbol{F}]_3 = \boldsymbol{F}(0,0),$$

and three edges, *i.e.*,

$$\begin{aligned} e_1 &= [\boldsymbol{F}]_{1,2} := \{\boldsymbol{F}(1-\xi,\xi) \,:\; \xi \in [0,1]\},\\ e_2 &= [\boldsymbol{F}]_{2,3} := \{\boldsymbol{F}(0,1-\xi) \,:\; \xi \in [0,1]\},\\ e_3 &= [\boldsymbol{F}]_{3,1} := \{\boldsymbol{F}(\xi,0) \,:\; \xi \in [0,1]\}, \end{aligned}$$

which are parametrized by polynomial curves of degree 2, *i.e.*, curves from $\mathbb{P}^1_2 \times \mathbb{P}^1_2$, where $\mathbb{P}^1_d$ denotes the space of univariate polynomials of degree at most $d \in \mathbb{N}_0$.

A special case of a quadratic triangle is the standard triangle obtained when $\boldsymbol{F} \in \mathbb{P}^2_1 \times \mathbb{P}^2_1$. In this case $\boldsymbol{F}$ is an affine mapping. It is uniquely determined by $\boldsymbol{V}_1, \boldsymbol{V}_2, \boldsymbol{V}_3$ as

$$\boldsymbol{F}(u,v) = u\boldsymbol{V}_1 + v\boldsymbol{V}_2 + (1-u-v)\boldsymbol{V}_3. \tag{1}$$

For a fixed $(u,v) \in \mathbb{R}^2$, the values u, v, $1-u-v$ correspond to the barycentric coordinates of the point $\boldsymbol{F}(u,v)$ with respect to the triangle defined by the vertices $\boldsymbol{V}_1$, $\boldsymbol{V}_2$, $\boldsymbol{V}_3$.

A quadratic triangulation is a collection of quadratic triangles, each of which is specified by its unique parametrization.

Definition 2 (*Quadratic Triangulation*)**.** For $M \in \mathbb{N}$, let $T^{(m)}$, $m = 1,2,\dots,M$, be quadratic triangles parametrized by $\boldsymbol{F}^{(m)} \in \mathbb{P}^2_2 \times \mathbb{P}^2_2$. The set $\mathcal{T} = \left\{T^{(1)}, T^{(2)}, \dots, T^{(M)}\right\}$ is a quadratic triangulation provided that the union of the quadratic triangles in $\mathcal{T}$ is connected, and the intersection of any two different quadratic triangles of $\mathcal{T}$ that have a non-empty intersection is either a vertex or an edge of these two quadratic triangles.

Suppose Ω is a planar domain, and $\mathcal{T}$ is a quadratic triangulation such that $\bigcup_{m=1}^{M} T^{(m)} = \Omega$. We then say that $\mathcal{T}$ is a triangulation of Ω. Note that in general the boundary of Ω is parametrized by a set of closed C^0 quadratic spline curves with no intersections.

For a given quadratic triangulation $\mathcal{T}$, we denote by $\mathcal{V}$ the set of vertices of all quadratic triangles in $\mathcal{T}$, *i.e.*,

$$\mathcal{V} = \bigcup_{m=1}^{M} \left\{[\boldsymbol{F}^{(m)}]_1, [\boldsymbol{F}^{(m)}]_2, [\boldsymbol{F}^{(m)}]_3\right\},$$

and denote the individual vertices in $\mathcal{V}$ by $\boldsymbol{V}_i$, $i = 1,2,\dots|\mathcal{V}|$. Similarly, we denote by $\mathcal{E}$ the set of edges of all quadratic triangles in $\mathcal{T}$, *i.e.*,

$$\mathcal{E} = \bigcup_{m=1}^{M} \left\{[\boldsymbol{F}^{(m)}]_{1,2}, [\boldsymbol{F}^{(m)}]_{2,3}, [\boldsymbol{F}^{(m)}]_{3,1}\right\},$$

and denote the individual edges in $\mathcal{E}$ by e_k, $k = 1,2,\dots|\mathcal{E}|$. We further split the set $\mathcal{E}$ into the set $\mathcal{E}_{\mathrm{I}}$ of interior edges shared by two quadratic triangles, and boundary edges $\mathcal{E}_{\mathrm{B}} = \mathcal{E} \setminus \mathcal{E}_{\mathrm{I}}$.

With respect to definitions, an edge of a quadratic triangulation is a set of points parametrized by a restriction of the parametrization that determines the quadratic triangle possessing this edge. For an interior edge, there are two triangles that have the edge in common, and we have to be aware of the fact that the induced parametrizations of the edge may have opposite directions. To take this into account, we define some further notation related to an edge.

Definition 3 (*Edge Direction*). Let $e_k \in \mathcal{E}$ be an edge connecting the vertices $\boldsymbol{V}_{i_1}, \boldsymbol{V}_{i_2} \in \mathcal{V}$. The direction of e_k from $\boldsymbol{V}_{i_1}$ to $\boldsymbol{V}_{i_2}$ is specified by expressing e_k as $[\boldsymbol{V}_{i_1}, \boldsymbol{V}_{i_2}]$. Suppose $T^{(m)} = [\boldsymbol{F}^{(m)}] \in \mathcal{T}$ is a quadratic triangle with the edge e_k, and let $(\ell_1, \ell_2) \in \{(1,2),(2,1),(2,3),(3,2),(3,1),(1,3)\}$ be such that $\boldsymbol{V}_{i_1} = [\boldsymbol{F}^{(m)}]_{\ell_1}$ and $\boldsymbol{V}_{i_2} = [\boldsymbol{F}^{(m)}]_{\ell_2}$. The direction $\mathrm{dir}_k^{(m)} \in \{-1, 1\}$, the edge parametrization $\boldsymbol{p}_k^{(m)} \in \mathbb{P}_1^1 \times \mathbb{P}_1^1$, and the direction vector $\boldsymbol{\sigma}_k^{(m)} = \frac{d}{d\xi}\boldsymbol{p}_k^{(m)}(\xi) \in \{-1,0,1\} \times \{-1,0,1\}$ in $\triangle$ of e_k with respect to $T^{(m)}$ are then given by

$$\left\{ \mathrm{dir}_k^{(m)}, \boldsymbol{p}_k^{(m)}(\xi), \boldsymbol{\sigma}_k^{(m)} \right\} = \begin{cases} \{1, (1-\xi, \xi), (-1, 1)\} & \text{if } (\ell_1, \ell_2) = (1,2), \\ \{-1, (\xi, 1-\xi), (1, -1)\} & \text{if } (\ell_1, \ell_2) = (2,1), \\ \{1, (0, 1-\xi), (0, -1)\} & \text{if } (\ell_1, \ell_2) = (2,3), \\ \{-1, (0, \xi), (0, 1)\} & \text{if } (\ell_1, \ell_2) = (3,2), \\ \{1, (\xi, 0), (1, 0)\} & \text{if } (\ell_1, \ell_2) = (3,1), \\ \{-1, (1-\xi, 0), (-1, 0)\} & \text{if } (\ell_1, \ell_2) = (1,3). \end{cases} \tag{2}$$

2.2. Splines in the Bernstein–Bézier representation

We start this section by briefly reviewing the Bernstein–Bézier representation of polynomials, which is a common tool for constructing and analyzing splines on triangulations.

Let $d \in \mathbb{N}$. The space of univariate polynomials $\mathbb{P}_d^1$ is spanned by the Bernstein basis polynomials

$$B_r^d(\xi) = \frac{d!}{r!\,(d-r)!}\xi^r(1-\xi)^{d-r}, \quad r = 0, 1, \ldots, d.$$

These basis functions naturally generalize to two variables as

$$B_{r,l}^d(u,v) = \frac{d!}{r!\,l!\,(d-r-l)!}u^r v^l (1-u-v)^{d-r-l}, \quad (r,l) \in \mathbb{I}_d,$$

where

$$\mathbb{I}_d = \left\{ (r,l) \in \mathbb{N}_0^2 : \ 0 \le r + l \le d \right\}$$

denotes the index set of cardinality $\binom{d+2}{2}$. The functions $B_{r,l}^d$, $(r,l) \in \mathbb{I}_d$, form a basis of $\mathbb{P}_d^2$. Hence any polynomial $p \in \mathbb{P}_d^2$ can be uniquely expressed as

$$p(u,v) = \sum_{(r,l)\in\mathbb{I}_d} b_{r,l} B_{r,l}^d(u,v) \tag{3}$$

for some coefficients $b_{r,l} \in \mathbb{R}$. Note that $b_{r,l} = \frac{r}{d}$ implies $p(u,v) = u$ and $b_{r,l} = \frac{l}{d}$ implies $p(u,v) = v$, thus the points $(\frac{r}{d}, \frac{l}{d})$, $(r,l) \in \mathbb{I}_d$, are called the domain points in $\triangle$.

A polynomial p in the form (3) can be computed by the de Casteljau algorithm, which is provided in Algorithm 1 (`DeCast`) in its extended version. It holds that

$$p(u,v) = \texttt{DeCast}\left(\left\{ b_{r,l},\ (r,l) \in \mathbb{I}_d \right\}, \left\{ (u,v)^{\langle d \rangle} \right\} \right),$$

where $(u,v)^{\langle d \rangle}$ denotes that (u,v) is repeated d times.

Remark 1. Another interesting aspect of Algorithm 1 is that the values $c_{r,l}$, $(r,l) \in \mathbb{I}_d$, computed as

$$c_{r,l} = \texttt{DeCast}\left(\left\{ b_{r',l'},\ (r',l') \in \mathbb{I}_d \right\}, \left\{ \boldsymbol{V}_1^{\langle r \rangle}, \boldsymbol{V}_2^{\langle l \rangle}, \boldsymbol{V}_3^{\langle d-r-l \rangle} \right\} \right)$$

for any three distinct noncollinear points $\boldsymbol{V}_1, \boldsymbol{V}_2, \boldsymbol{V}_3 \in \mathbb{R}^2$, determine the coefficients of $p \circ \boldsymbol{F}$, *i.e.*,

$$p(\boldsymbol{F}(u,v)) = \sum_{(r,l)\in\mathbb{I}_d} c_{r,l} B_{r,l}^d(u,v),$$

where $\boldsymbol{F}$ is given by (1).

Let us now consider a bounded domain $\Omega \subset \mathbb{R}^2$ that is partitioned by a quadratic triangulation $\mathcal{T} = \left\{ T^{(1)}, T^{(2)}, \ldots, T^{(M)} \right\}$. Recall from Definition 2 that each quadratic triangle $T^{(m)}$, $m \in \{1, 2, \ldots, M\}$, is determined by a local parametrization $\boldsymbol{F}^{(m)}$. In the Bernstein–Bézier representation it can be expressed as

$$\boldsymbol{F}^{(m)}(u,v) = \sum_{(r,l)\in\mathbb{I}_2} \boldsymbol{C}_{r,l}^{(m)} B_{r,l}^2(u,v), \tag{4}$$

where $\boldsymbol{C}_{r,l}^{(m)} \in \mathbb{R}^2$ represent control points. On $\mathcal{T}$ we define the vector space of splines of degree $d \in \mathbb{N}$ and smoothness $r \in \mathbb{N}_0$ by

$$\mathbb{S}_d^r(\mathcal{T}) := \left\{ \varphi \in C^r(\Omega) : \ \varphi|_{T^{(m)}} \circ \boldsymbol{F}^{(m)} \in \mathbb{P}_d^2 \text{ for every } T^{(m)} \in \mathcal{T} \right\}. \tag{5}$$

Algorithm 1: De Casteljau algorithm (`DeCast`)

Input: Bézier ordinates $c_{r,l}$, $(r,l) \in \mathbb{I}_d$, coordinates $(u_1, v_1), (u_2, v_2), \dots, (u_d, v_d)$

$c^{(0)}_{(r,l)} \leftarrow c_{r,l}$, $(r,l) \in \mathbb{I}_d$;

for $t = 1, 2, \dots, d$ **do**

  foreach $(r,l) \in \mathbb{I}_{d-t}$ **do**

    $c^{(t)}_{(r,l)} \leftarrow u_t c^{(t-1)}_{(r+1,l)} + v_t c^{(t-1)}_{(r,l+1)} + (1 - u_t - v_t) c^{(t-1)}_{(r,l)}$;

  end

end

Output: value $c^{(d)}_{(0,0)}$

If $\mathcal{T}$ is a linear triangulation, *i.e.*, $\boldsymbol{F}^{(m)} \in \mathbb{P}^2_1 \times \mathbb{P}^2_1$ for every $T^{(m)} \in \mathcal{T}$, this definition agrees with the standard definition of polynomial splines over a triangulation. Indeed, for a linear triangulation the restriction $\varphi|_{T^{(m)}}$ of a spline $\varphi \in \mathbb{S}^r_d(\mathcal{T})$ to any $T^{(m)} \in \mathcal{T}$ is a polynomial in $\mathbb{P}^2_d$ since the inverse of $\boldsymbol{F}^{(m)}$ is in $\mathbb{P}^2_1 \times \mathbb{P}^2_1$. For a general $\boldsymbol{F}^{(m)} \in \mathbb{P}^2_2 \times \mathbb{P}^2_2$, however, this does not hold.

As for the linear triangulations, the space of continuous splines $\mathbb{S}^0_d(\mathcal{T})$ over a quadratic triangulation $\mathcal{T}$ is simple to analyze. Its dimension

$$\dim\left(\mathbb{S}^0_d(\mathcal{T})\right) = |\mathcal{V}| + (d-1)|\mathcal{E}| + \binom{d-1}{2}|\mathcal{T}|$$

is independent of the parametrizations of the quadratic triangles. For higher orders of smoothness this is no longer true.

2.3. C^1 smoothness conditions

In this section we summarize the results derived in [17] that, for a spline defined over a quadratic triangulation, provide C^1 smoothness conditions along an edge shared by two quadratic triangles.

Let $T^{(m_1)}, T^{(m_2)} \in \mathcal{T}$ be two quadratic triangles sharing an edge $e_k \in \mathcal{E}_1$. Assume that the geometry mappings $\boldsymbol{F}^{(m_1)}$ and $\boldsymbol{F}^{(m_2)}$ are quadratic as defined in (4), and that the edge is parametrized as

$$e_k = \left\{ \boldsymbol{F}^{(m_1)}\left(\boldsymbol{p}^{(m_1)}_k(\xi)\right) = \boldsymbol{F}^{(m_2)}\left(\boldsymbol{p}^{(m_2)}_k(\xi)\right) : \ \xi \in [0,1] \right\}, \tag{6}$$

where we use the notation (2) introduced in Definition 3. Note that we consider points as row vectors. With the edge e_k we associate the mapping $\boldsymbol{t}_k : [0,1] \to \mathbb{R}^2$ defined by

$$\boldsymbol{t}_k(\xi) = \boldsymbol{\sigma}^{(m_1)}_k \cdot \left(\boldsymbol{J}\boldsymbol{F}^{(m_1)}(\boldsymbol{p}^{(m_1)}_k(\xi))\right)^T = \boldsymbol{\sigma}^{(m_2)}_k \cdot \left(\boldsymbol{J}\boldsymbol{F}^{(m_2)}(\boldsymbol{p}^{(m_2)}_k(\xi))\right)^T. \tag{7}$$

To each parameter $\xi \in [0,1]$, this mapping assigns the tangent vector $\boldsymbol{t}_k(\xi)$ corresponding to the parametrization (6). Similarly, let $\boldsymbol{n}_k : [0,1] \to \mathbb{R}^2$ be the mapping that assigns to each $\xi \in [0,1]$ the normal vector $\boldsymbol{n}_k(\xi)$ of the edge parametrization. We can express it as

$$\boldsymbol{n}_k(\xi) = \boldsymbol{t}_k(\xi)^{\perp}, \tag{8}$$

where $(x,y)^{\perp} = (y,-x)$ for $(x,y) \in \mathbb{R}^2$.

For a spline $\varphi \in S^0_d(\mathcal{T})$, let $\varphi^{(\ell)} = \varphi\big|_{T^{(\ell)}}$, $\ell \in \{m_1, m_2\}$, be the restriction of φ to $T^{(\ell)}$. By (5) the function $f^{(\ell)} = \varphi^{(\ell)} \circ \boldsymbol{F}^{(\ell)}$ is in $\mathbb{P}^2_d$. Let us consider the values of $\varphi^{(\ell)}$ on e_k. A point $(x,y) \in e_k$ can be expressed as $(x,y) = \boldsymbol{F}^{(\ell)}(u,v)$ with $(u,v) = \boldsymbol{p}^{(\ell)}_k(\xi)$. Let $\theta_k \in \mathbb{P}^1_d$ denote the trace function associated with e_k, *i.e.*, the polynomial that we consider on the interval $[0,1]$ and is given by

$$\theta_k(\xi) = f^{(m_1)}\left(\boldsymbol{p}^{(m_1)}_k(\xi)\right) = f^{(m_2)}\left(\boldsymbol{p}^{(m_2)}_k(\xi)\right). \tag{9}$$

The expression is well-defined since φ is continuous.

To derive conditions for C^1 smoothness of φ across e_k, we must investigate the normal derivatives of φ along e_k. Let $\nabla\varphi^{(\ell)}(x,y)$ be the gradient of $\varphi^{(\ell)}$ at (x,y) considered as a row vector. We observe that

$$\nabla\varphi^{(\ell)}(x,y) = \nabla f^{(\ell)}(u,v) \cdot \left(\boldsymbol{J}\boldsymbol{F}^{(\ell)}(u,v)\right)^{-1} = \nabla f^{(\ell)}(u,v) \cdot \boldsymbol{Q}^{(\ell)}_k \cdot \left(\boldsymbol{J}\boldsymbol{F}^{(\ell)}(u,v) \cdot \boldsymbol{Q}^{(\ell)}_k\right)^{-1},$$

where we introduce the matrix

$$\boldsymbol{Q}^{(\ell)}_k = \left(\left(\boldsymbol{\sigma}^{(\ell)\perp}_k\right)^T, \left(\boldsymbol{\sigma}^{(\ell)}_k\right)^T\right) \in \mathbb{R}^{2\times 2}$$

determined by the edge direction vector $\boldsymbol{\sigma}^{(\ell)}_k$, defined in (2). Note that $\boldsymbol{\sigma}^{(\ell)\perp}_k = \left(\boldsymbol{\sigma}^{(\ell)}_k\right)^{\perp}$.

A short calculation reveals that

$$\left(\boldsymbol{J}\boldsymbol{F}^{(\ell)}(u,v)\cdot\boldsymbol{Q}_k^{(\ell)}\right)^{-1}=\frac{1}{\det\left(\boldsymbol{Q}_k^{(\ell)}\right)\det(\mathrm{J}\boldsymbol{F}^{(\ell)}(u,v))}\begin{pmatrix}\left(\boldsymbol{\sigma}_k^{(\ell)}\cdot\left(\boldsymbol{J}\boldsymbol{F}^{(\ell)}(u,v)\right)^T\right)^{\perp}\\-\left(\boldsymbol{\sigma}_k^{(\ell)\perp}\cdot\left(\boldsymbol{J}\boldsymbol{F}^{(\ell)}(u,v)\right)^T\right)^{\perp}\end{pmatrix}.$$

By some further computation taking into account (7) and (8) we obtain

$$D_{\boldsymbol{n}_k(\xi)}\varphi^{(\ell)}(x,y)=\frac{1}{\alpha_k^{(\ell)}(\xi)}\left(\beta_k(\xi)\left\langle\nabla f^{(\ell)}(u,v),\,\boldsymbol{\sigma}_k^{(\ell)\perp}\right\rangle-\beta_k^{(\ell)}(\xi)\theta_k'(\xi)\right)\tag{10}$$

where

$$\alpha_k^{(\ell)}(\xi)=\left\|\boldsymbol{\sigma}_k^{(\ell)}\right\|^2\det\left(\mathrm{J}\boldsymbol{F}^{(\ell)}(u,v)\right),\quad\beta_k^{(\ell)}(\xi)=\left\langle\left(\boldsymbol{\sigma}_k^{(\ell)\perp}\cdot\left(\boldsymbol{J}\boldsymbol{F}^{(\ell)}(u,v)\right)^T\right)^{\perp},\,\boldsymbol{n}_k(\xi)\right\rangle,\quad\beta_k(\xi)=\left\|\boldsymbol{n}_k(\xi)\right\|^2.$$

The functions $\alpha_k^{(\ell)}$ and $\beta_k^{(\ell)}$ are polynomials of degree at most 2, and β_k is either a constant or a quadratic polynomial.

A spline $\varphi\in S_d^0(\mathcal{T})$ is C^1 smooth across e_k if and only if $D_{\boldsymbol{n}_k(\xi)}\varphi^{(m_1)}(x,y)=D_{\boldsymbol{n}_k(\xi)}\varphi^{(m_2)}(x,y)$ for every $(x,y)\in e_k$. Suppose $q_k\in\mathbb{P}_2^1$ is the greatest common divisor of $\alpha_k^{(m_1)}$ and $\alpha_k^{(m_2)}$. According to (10) the C^1 smoothness condition implies that $\widetilde{\alpha}_k^{(\ell)}=\alpha_k^{(\ell)}/q_k$ divides $\beta_k(\xi)\left\langle\nabla f^{(\ell)}(u,v),\,\boldsymbol{\sigma}_k^{(\ell)\perp}\right\rangle-\beta_k^{(\ell)}(\xi)\theta_k'(\xi)$, and hence $D_{\boldsymbol{n}_k(\xi)}\varphi^{(\ell)}(x,y)=\omega_k(\xi)/q_k(\xi)$ for some $\omega_k\in\mathbb{P}_{d+1}^1$. Using (10) again, it is easy to check that φ is C^1 smooth across e_k if and only if

$$\beta_k(\xi)\left\langle\nabla f^{(\ell)}\left(\boldsymbol{p}_k^{(\ell)}(\xi)\right),\,\boldsymbol{\sigma}_k^{(\ell)\perp}\right\rangle=\beta_k^{(\ell)}(\xi)\theta_k'(\xi)+\widetilde{\alpha}_k^{(\ell)}(\xi)\omega_k(\xi),\quad\ell\in\{m_1,m_2\},\quad\xi\in[0,1].\tag{11}$$

As the left-hand side of this condition is a polynomial of degree at most $d-1+\deg(\beta_k)$, the same must hold for the right-hand side, which additionally must be divisible by β_k. So, clearly, this implies certain restrictions on the choice of $\theta_k\in\mathbb{P}_d^1$ and $\omega_k\in\mathbb{P}_{d+1}^1$. The analysis of this problem can be found in [17]. In what follows we briefly review the key points and accompany them with Algorithm 2 provided in the appendix.

For every edge e_k, Algorithm 2 computes the functions θ_k and ω_k, the polynomials

$$\eta_k^{(\ell)}(\xi)=\left\langle\nabla f^{(\ell)}\left(\boldsymbol{p}_k^{(\ell)}(\xi)\right),\,\boldsymbol{\sigma}_k^{(\ell)\perp}\right\rangle,\quad\xi\in[0,1],\quad\ell\in\{m_1,m_2\},\tag{12}$$

and a list of all free parameters associated with the edge e_k. The degrees of freedom associated with ω_k depend on the constant d_k, defined by

$$d_k=d-1-\max\left\{\deg\left(\alpha_k^{(m_1)}\right),\deg\left(\alpha_k^{(m_2)}\right)\right\}+\deg(q_k),\tag{13}$$

that can attain values $d_k\in\{d-3,d-2,d-1\}$. The lowest value $d-3$ represents the generic case. The degree can be higher only in some special cases, *i.e.*, when $\alpha_k^{(m_1)},\alpha_k^{(m_2)}\in\mathbb{P}_2^1$ have a nonconstant common factor q_k or when they are both of degree less than 2. To highlight possible additional degrees of freedom, we associate with the edge e_k the value $\chi_k=d_k-(d-3)\in\{0,1,2\}$.

The Algorithm 2 takes into account the following possible parametrizations of e_k.

- If the edge e_k is a parabola, then β_k is an irreducible quadratic polynomial and the polynomials θ_k and ω_k are of the form

$$\theta_k(\xi)=\vartheta_0+\int_0^{\xi}\left(\tau^*(t)\beta_k(t)+\hat{\tau}(t)\right)dt,\quad\omega_k(\xi)=\omega^*(\xi)\beta_k(\xi)+\hat{\omega}(\xi),\tag{14}$$

  where $\vartheta_0\in\mathbb{R}$ is a free constant and the polynomials $\tau^*\in\mathbb{P}_{d-3}^1$ and $\omega^*\in\mathbb{P}_{d_k}^1$ are free to choose, whereas the polynomials $\hat{\tau},\hat{\omega}\in\mathbb{P}_1^1$ are not mutually independent but can be expressed with two free parameters. For more details, see Algorithm 3 in the appendix. From this algorithm it follows that $\hat{\tau}$ and $\hat{\omega}$ are of the form

$$\hat{\tau}(\xi)=\mu_1\hat{\tau}_0(\xi)+\mu_2\hat{\tau}_1(\xi),\quad\hat{\omega}(\xi)=\mu_1\hat{\omega}_0(\xi)+\mu_2\hat{\omega}_1(\xi)$$

  for any two constants μ_1, μ_2. The polynomials $\hat{\tau}_0,\hat{\tau}_1,\hat{\omega}_0,\hat{\omega}_1\in\mathbb{P}_1^1$ are determined by the geometry mappings. Moreover, the polynomial $\hat{\tau}_0$ is always nonzero, and at least one of the polynomials $\hat{\tau}_1$, $\hat{\omega}_1$ is nonzero. So the parameter μ_1 represents one additional degree of freedom associated with θ_k, and μ_2 is associated with a combination of θ_k' and ω_k (equivalently, with a directional derivative in any direction that is parallel neither to the trace nor to the normal direction).
  Finally, let us count the number of parameters that can be associated with θ_k and ω_k. If we express τ^* in the basis of the Bernstein polynomials of degree $d-3$ and use the fact that the polynomials $\beta_kB_0^{d-3},\beta_kB_1^{d-3},\dots,\beta_kB_{d-3}^{d-3}$ are linearly independent and of degree at least 2, we see that these polynomials and $\hat{\tau}$ are linearly independent. After the integration, this means that θ_k lies in a polynomial subspace spanned by (at least) d linearly independent polynomials, *i.e.*, there are d degrees of freedom for constructing θ_k (without using μ_2). By the same line of arguments we see that there are always $d_k+1=d-2+\chi_k$ independent parameters for constructing ω_k (without using μ_1 and μ_2).
- If the edge e_k is a non-uniformly parametrized straight line, then β_k is a square of a linear polynomial, *i.e.*, $\beta_k(\xi)=\zeta^2(\xi)$ for some $\zeta\in\mathbb{P}_1^1$. This may be considered as a special example of the previous case, and the polynomials θ_k and ω_k can again be represented in the form (14). The polynomial ζ divides $\alpha_k^{(m_1)}$ and $\alpha_k^{(m_2)}$, hence the lowest value for d_k is $d-2$, *i.e.*, $\chi_k\geq1$. Moreover, taking $\hat{\tau}(\xi)=\mu_1\zeta(\xi)$ for $\mu_1\in\mathbb{R}$ and $\hat{\omega}(\xi)=0$ ensures C^1 smoothness; see Algorithm 3. This gives d degrees of freedom associated with θ_k and $d_k+1\geq d-1$ degrees of freedom associated with ω_k. A special edge case that provides an additional degree of freedom is covered in [17, Proposition 5].

- If the edge e_k is a uniformly parametrized straight line, then β_k is a constant. A sufficient condition for C^1 smoothness is to choose $\theta_k \in \mathbb{P}^1_{d-1}$ and $\omega_k \in \mathbb{P}^1_{d_k}$, where d_k is again defined by (13) and is either equal to $d-2$ or $d-1$, *i.e.*, $\chi_k \geq 1$. Additionally, there exists a special geometric configuration (see Algorithm 2), in which we can choose $\theta_k \in \mathbb{P}^1_d$ and $\omega_k \in \mathbb{P}^1_{d_k+1}$ and impose a linear constraint on the leading coefficients of θ_k and ω_k.

To summarize all cases, there are $2d-1$, $2d$, or $2d+1$ independent free parameters associated with e_k. More specifically, there are

- d or $d+1$ free parameters associated with θ_k that we collect in the set $\mathbf{par}^e_{k,1}$;
- $d-2+\chi_k$, $\chi_k \in \{0,1,2\}$, free parameters associated with ω_k that we collect in the set $\mathbf{par}^e_{k,2}$;
- one possible additional free parameter associated with a combination of θ'_k and ω_k that we collect in the set $\mathbf{par}^e_{k,3}$.

The sets $\mathbf{par}^e_{k,1}$, $\mathbf{par}^e_{k,2}$, $\mathbf{par}^e_{k,3}$ are among the outputs of Algorithm 3.

Remark 2. As observed, the number of degrees of freedom associated with an edge in a generic case is equal to $2d-1$. However, for certain special configurations of mesh elements, we may obtain up to two additional free parameters. This for example happens when the geometry mappings are C^1 smooth along the edge or the geometry mappings are linear. For linear elements the number of degrees of freedom is always $2d+1$ (see [18]), which is the main difference between splines on (linear) triangulations and quadratic triangulations.

Enforcing C^1 smoothness at the vertices of a triangulation brings the same challenges in both linear and quadratic settings. To ensure that the dimension is independent on the geometry of the mesh at the vertices, one can either require higher order of smoothness (super-smoothness) at vertices or use macro-element splitting techniques. In this work, we opt for the Clough–Tocher refinement.

3. Clough–Tocher spline spaces on a quadratic triangulation

In this section we establish a C^1 smooth spline space on a quadratic triangulation of any degree greater than or equal to four. We show how to employ Clough–Tocher splitting technique on quadratic Bézier triangles and identify degrees of freedom of a spline defined on the induced partition. We describe interpolation problems that characterize the considered spaces, introduce basis functions based on interpolation functionals and provide some numerical examples.

3.1. Clough–Tocher refinement

Let $T^{(m)}$ be a quadratic triangle of a given quadratic triangulation $\mathcal{T}$, and let $\boldsymbol{F}^{(m)}$ be its corresponding parametrization specified as in (4). In order to facilitate the construction of C^1 splines over $\mathcal{T}$ we split $T^{(m)}$ into three smaller quadratic triangles by choosing a split point $\boldsymbol{v}_{\mathrm{ct}}$ in the interior of $\triangle$. As it is common, we choose $\boldsymbol{v}_{\mathrm{ct}}$ to be the barycenter of $\triangle$, *i.e.*, $\boldsymbol{v}_{\mathrm{ct}} = (\frac{1}{3}, \frac{1}{3})$. We then subdivide the quadratic mapping $\boldsymbol{F}^{(m)}$ to three triangles:

- the triangle determined by the vertices $(1,0)$, $(0,1)$, $\boldsymbol{v}_{\mathrm{ct}}$;
- the triangle determined by the vertices $(0,1)$, $(0,0)$, $\boldsymbol{v}_{\mathrm{ct}}$;
- the triangle determined by the vertices $(0,0)$, $(1,0)$, $\boldsymbol{v}_{\mathrm{ct}}$.

Following Remark 1, this defines three new quadratic geometry mappings $\boldsymbol{F}^{(m)}_\ell : \triangle \to \mathbb{R}^2$, $\ell = 1,2,3$, given by

$$\boldsymbol{F}^{(m)}_\ell(u,v) = \sum_{(r,l)\in\mathbb{I}_2} \boldsymbol{C}^{(m,\ell)}_{r,l} B^2_{r,l}(u,v)$$

with control points $\boldsymbol{C}^{(m,\ell)}_{r,l} \in \mathbb{R}^2$ that can be obtained using Algorithm 1 as

$$\begin{aligned}
\boldsymbol{C}^{(m,1)}_{r,l} &= \texttt{DeCast}\left(\left\{\boldsymbol{C}^{(m)}_{r',l'}, (r',l') \in \mathbb{I}_2\right\}, \left\{(1,0)^{\langle r\rangle}, (0,1)^{\langle l\rangle}, \boldsymbol{v}_{\mathrm{ct}}^{\langle d-r-l\rangle}\right\}\right),\\
\boldsymbol{C}^{(m,2)}_{i,j} &= \texttt{DeCast}\left(\left\{\boldsymbol{C}^{(m)}_{r',l'}, (r',l') \in \mathbb{I}_2\right\}, \left\{(0,1)^{\langle r\rangle}, (0,0)^{\langle l\rangle}, \boldsymbol{v}_{\mathrm{ct}}^{\langle d-r-l\rangle}\right\}\right),\\
\boldsymbol{C}^{(m,3)}_{r,l} &= \texttt{DeCast}\left(\left\{\boldsymbol{C}^{(m)}_{r',l'}, (r',l') \in \mathbb{I}_2\right\}, \left\{(0,0)^{\langle r\rangle}, (1,0)^{\langle l\rangle}, \boldsymbol{v}_{\mathrm{ct}}^{\langle d-r-l\rangle}\right\}\right).
\end{aligned}$$

In this way we define the splitting of each macro quadratic triangle $T^{(m)}$ into three micro quadratic triangles $T^{(m)}_\ell = [\boldsymbol{F}^{(m)}_\ell]$; see Fig. 2 for an illustration.

The described splitting of each quadratic triangle $T^{(m)} \in \mathcal{T}$ induces the Clough–Tocher refinement

$$\mathcal{T}_{\mathrm{CT}} = \bigcup_{m=1}^{M} \left\{T^{(m)}_1, T^{(m)}_2, T^{(m)}_3\right\}$$

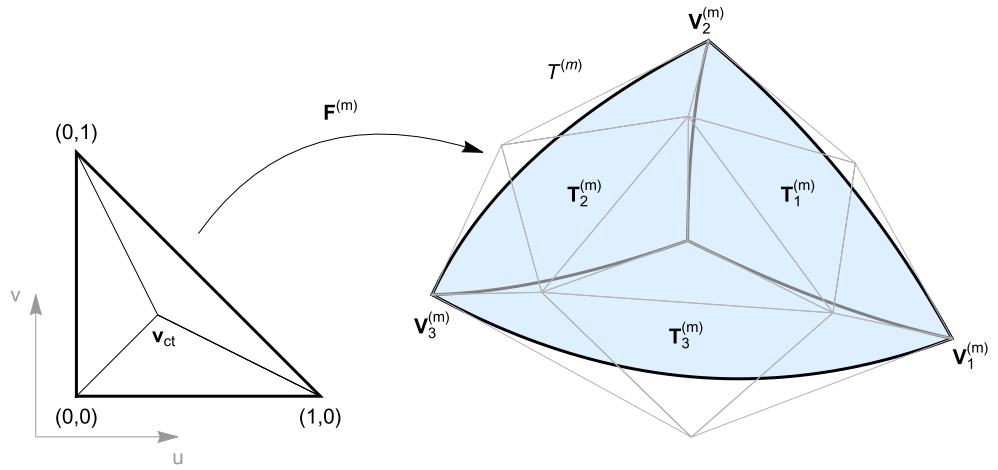

Fig. 2. The Clough–Tocher refinement of a quadratic triangle $T^{(m)}$ parametrized by $\boldsymbol{F}^{(m)}$ into three quadratic triangles $T_\ell^{(m)}$, $\ell = 1, 2, 3$, obtained by subdividing $\boldsymbol{F}^{(m)}$.

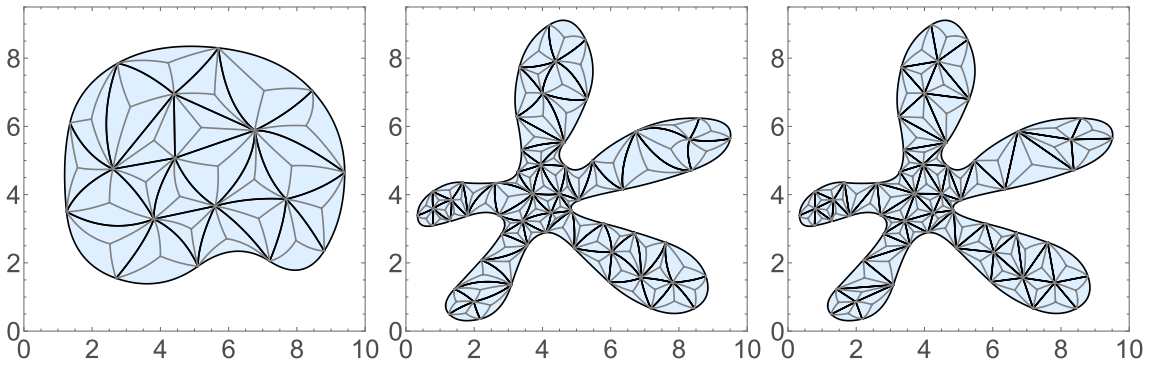

Fig. 3. Examples of Clough–Tocher refined quadratic triangulations.

of $\mathcal{T}$, *i.e.*, a quadratic triangulation consisting of $3M$ triangles; see Fig. 3 for some examples. Let $\mathcal{V}_{\text{ct}}$ denote the set of triangle split points $\boldsymbol{V}_{\text{ct}}^{(m)} = \boldsymbol{F}^{(m)}(\boldsymbol{v}_{\text{ct}})$, $m = 1, 2, \dots, M$. The vertex set of $\mathcal{T}_{\text{CT}}$ is $\mathcal{V}_{\text{CT}} = \mathcal{V} \cup \mathcal{V}_{\text{ct}}$. Moreover, let

$$\mathcal{E}_{\text{ct}} = \bigcup_{m=1}^{M} \left\{ \left[\boldsymbol{F}_1^{(m)}\right]_{3,1}, \left[\boldsymbol{F}_2^{(m)}\right]_{3,1}, \left[\boldsymbol{F}_3^{(m)}\right]_{3,1} \right\}$$

be the set of newly introduced edges. Then the edge set of $\mathcal{T}_{\text{CT}}$ equals $\mathcal{E}_{\text{CT}} = \mathcal{E} \cup \mathcal{E}_{\text{ct}}$.

We fix some further notation related to the edges in $\mathcal{E}$. For $T^{(m)} \in \mathcal{T}$, let

$$e_1^{(m)} = \left[\boldsymbol{F}^{(m)}\right]_{1,2} = \left[\boldsymbol{F}_1^{(m)}\right]_{1,2}, \quad e_2^{(m)} = \left[\boldsymbol{F}^{(m)}\right]_{2,3} = \left[\boldsymbol{F}_2^{(m)}\right]_{1,2}, \quad e_3^{(m)} = \left[\boldsymbol{F}^{(m)}\right]_{3,1} = \left[\boldsymbol{F}_3^{(m)}\right]_{1,2}. \tag{15}$$

Notice that for parametrizations $\boldsymbol{F}_1^{(m)}$, $\boldsymbol{F}_2^{(m)}$, $\boldsymbol{F}_3^{(m)}$ these edges are connecting the vertices at positions 1 and 2. For every interior edge $e_k \in \mathcal{E}_{\text{I}}$, let $T_{\ell_1}^{(m_1)}$ and $T_{\ell_2}^{(m_2)}$ be the triangles in $\mathcal{T}_{\text{CT}}$ with the edge e_k in common, *i.e.*, $e_k = e_{\ell_1}^{(m_1)} = e_{\ell_2}^{(m_2)}$. So, recalling Definition 3, for every edge $e_k \in \mathcal{E}_{\text{I}}$ we have that

$$e_k = \left\{ \boldsymbol{F}_{\ell_1}^{(m_1)}\left(\boldsymbol{p}_k^{(m_1)}(\xi)\right) = \boldsymbol{F}_{\ell_2}^{(m_2)}\left(\boldsymbol{p}_k^{(m_2)}(\xi)\right) : \ \xi \in [0,1] \right\}, \tag{16a}$$

where

$$\boldsymbol{p}_k^{(m_j)}(\xi) = \begin{cases} (1-\xi, \xi) & \text{if } \text{dir}_k^{(m_j)} = 1, \\ (\xi, 1-\xi) & \text{if } \text{dir}_k^{(m_j)} = -1, \end{cases} \qquad j = 1, 2. \tag{16b}$$

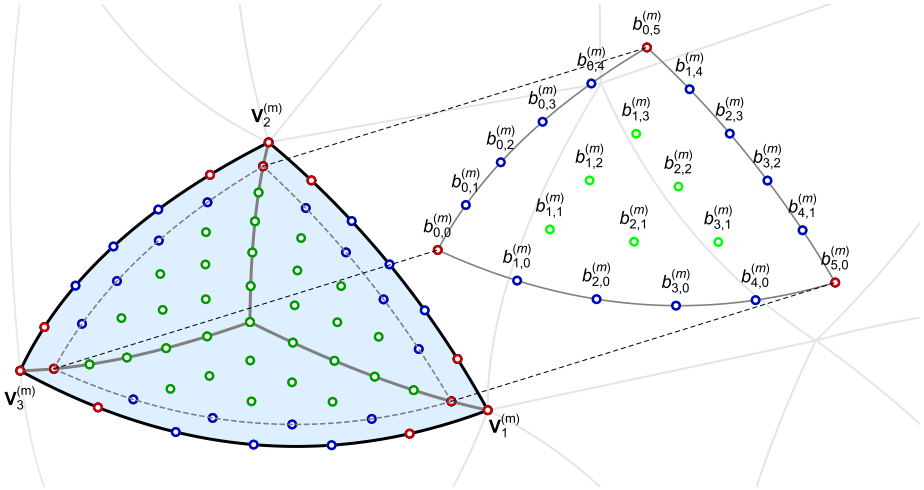

Fig. 4. A Clough–Tocher refined quadratic triangle $T^{(m)} \in \mathcal{T}$ (depicted in blue) with vertices $\boldsymbol{V}_\ell^{(m)}$, $\ell = 1,2,3$, and the associated domain points of degree 6. The coefficients corresponding to the red colored domain points form the vertex group, the coefficients corresponding to the blue colored domain points form the edge group, and the coefficients corresponding to the green colored domain points form the triangle group of $T^{(m)}$. The values associated with the domain points located inside the blue colored region bounded by dashed points can be interpreted as coefficients of a degree 5 polynomial after subdivision, which is schematically depicted in the right part of the figure.

3.2. Spline spaces

For $d \geq 4$, let $\mathbb{S}_d^1(\mathcal{T}_{\mathrm{CT}})$ be the C^1 smooth spline space on the refined triangulation $\mathcal{T}_{\mathrm{CT}}$ as defined in (5). We are interested in its subspace

$$\mathbb{S}_d(\mathcal{T}_{\mathrm{CT}}) := \mathbb{S}_d^1(\mathcal{T}_{\mathrm{CT}}) \cap C^{d-1}(\mathcal{V}_{\mathrm{ct}}). \tag{17}$$

The super-smoothness of order $d-1$ at the triangle split points significantly reduces the dimension of the space and conceals the effect of the artificial splitting inside a macro triangle. Note that by imposing super-smoothness of order d instead of $d-1$ we would obtain the space $\mathbb{S}_d^1(\mathcal{T})$.

Let us consider a spline $\varphi \in \mathbb{S}_d(\mathcal{T}_{\mathrm{CT}})$ on a triangle $T^{(m)} \in \mathcal{T}$. Similarly as in Section 2.3, let $\varphi^{(m)} = \varphi\big|_{T^{(m)}}$ denote the restriction of φ to $T^{(m)}$ and $\varphi_\ell^{(m)} = \varphi\big|_{T_\ell^{(m)}}$, $\ell = 1,2,3$, the restrictions of φ to the refined triangles $T_\ell^{(m)}$. Moreover, let $f^{(m)} = \varphi^{(m)} \circ \boldsymbol{F}^{(m)}$, and let the polynomials $f_\ell^{(m)} = \varphi_\ell^{(m)} \circ \boldsymbol{F}_\ell^{(m)} \in \mathbb{P}_d^2$ be expressed in the form

$$f_\ell^{(m)}(u,v) = \sum_{(r,l)\in\mathbb{I}_d} c_{r,l}^{(m,\ell)} B_{r,l}^d(u,v) \tag{18}$$

for some $c_{r,l}^{(m,\ell)} \in \mathbb{R}$. These coefficients are not independent due to the smoothness requirements.

The problem of finding the subset of coefficients that uniquely determine all the others is known as the problem of finding a minimal determining set; see, *e.g.*, [2]. For this purpose we organize the coefficients related to $T^{(m)}$ into three groups (similarly as in [7] for the case of linear geometry mappings):

- the vertex group consists of the coefficients

$$c_{d,0}^{(m,\ell)}, c_{d-1,0}^{(m,\ell)}, c_{d-1,1}^{(m,\ell)}, \qquad c_{0,d}^{(m,\ell)}, c_{0,d-1}^{(m,\ell)}, c_{1,d-1}^{(m,\ell)}, \qquad \ell = 1,2,3; \tag{19}$$

- the edge group consists of the coefficients

$$c_{r,d-r}^{(m,\ell)},\ r = 2,3,\ldots,d-2, \qquad c_{r,d-1-r}^{(m,\ell)},\ r = 1,2,\ldots,d-2, \qquad \ell = 1,2,3; \tag{20}$$

- the triangle group consists of the coefficients

$$c_{r,l}^{(m,\ell)},\ r = 0,1,\ldots,d-2,\ l = 0,1,\ldots,d-2-r, \qquad \ell = 1,2,3. \tag{21}$$

Fig. 4 provides an example of these groups for degree $d = 6$. Each of the coefficients $c_{r,l}^{(m,\ell)}$, $(r,l) \in \mathbb{I}_d$, is associated with the domain point $\boldsymbol{F}_\ell^{(m)}(\frac{r}{d}, \frac{l}{d})$.

For a fixed $\ell \in \{1,2,3\}$ there are six coefficients in the vertex group that are related by C^1 smoothness conditions at the corresponding vertex of $T^{(m)}$. It is clear that they are all determined by three degrees of freedom, *e.g.*, by value and gradient of

the spline at the vertex. In fact, fixing these three degrees of freedom uniquely determines the associated coefficients in the vertex groups of all quadratic triangles of Δ that have this vertex in common.

Let us now consider the coefficients in the edge group corresponding to the edge $e_k = e_\ell^{(m)} \in \mathcal{E}$ for a fixed $\ell \in \{1,2,3\}$.

- If e_k is an interior edge, let $T_\ell^{(m)}$ and $T_{\ell'}^{(m')}$ be the triangles in $\mathcal{T}_{\mathrm{CT}}$ with the edge e_k in common, *i.e.*, $e_k = e_\ell^{(m)} = e_{\ell'}^{(m')}$. With the notation as in (16) we use Algorithm 2 to compute
$$\left\{\theta_k, \omega_k, \eta_k^{(m)}, \eta_k^{(m')}, \mathbf{par}_k^e\right\} = \mathtt{TrAndDer}\left(\boldsymbol{F}_\ell^{(m)}, \boldsymbol{F}_{\ell'}^{(m')}, \boldsymbol{p}_k^{(m)}, \boldsymbol{p}_k^{(m')}, d\right), \tag{22}$$
where $\mathbf{par}_k^e = \left\{\mathbf{par}_{k,1}^e, \mathbf{par}_{k,2}^e, \mathbf{par}_{k,3}^e\right\}$ collects free parameters corresponding to the trace θ_k, the normal derivative ω_k, and their combination, respectively.
- If e_k is a boundary edge, $T_\ell^{(m)}$ is the only triangle in $\mathcal{T}_{\mathrm{CT}}$ with the edge e_k. Nonetheless, we can make use of Algorithm 2 to produce the outputs of (22). First, we reflect the domain triangle over the line corresponding to e_k in the parameter domain. We define the geometry mapping $\boldsymbol{F}_{\ell'}^{(m')}$ by extrapolating the mapping $\boldsymbol{F}_\ell^{(m)}$ onto the reflected domain triangle, which gives rise to an artificial quadratic triangle that serves as $T_{\ell'}^{(m')}$. Then, we apply Algorithm 2 to compute (22) by using $\boldsymbol{F}_{\ell'}^{(m')} = \boldsymbol{F}_\ell^{(m)}$ and $\boldsymbol{p}_k^{(m')} = \boldsymbol{p}_k^{(m)}$. Consequently, the geometry mappings are smooth over e_k, and the number of degrees of freedom collected in $\mathbf{par}_k^e$ is $2d+1$. Since in this case the degree of freedom in $\mathbf{par}_{k,3}^e$ can be associated with θ_k, we set $\mathbf{par}_{k,1}^e \leftarrow \mathbf{par}_{k,1}^e \cup \mathbf{par}_{k,3}^e$, $\mathbf{par}_{k,3}^e \leftarrow \{\}$.

Remark 3. The computation of degrees of freedom and representation of the trace and directional derivative for every edge $e_k \in \mathcal{E}$ is completely local (it depends only on two quadratic triangles sharing the edge). It can be done in the preprocessing step and stored for later use.

With the help of (22) the C^1 smoothness conditions along $e_k = e_\ell^{(m)}$ induced by (9) and (12) can be expressed as
$$f_\ell^{(m)}\left(\boldsymbol{p}_k^{(m)}(\xi)\right) = \theta_k(\xi), \quad \left\langle \nabla f_\ell^{(m)}\left(\boldsymbol{p}_k^{(m)}(\xi)\right), \mathrm{dir}_k^{(m)}(1,1)\right\rangle = \eta_k^{(m)}(\xi), \quad \xi \in [0,1], \tag{23}$$
where by (16) we have that $\boldsymbol{p}_k^{(m)}(\xi) = (1-\xi, \xi)$ and $\mathrm{dir}_k^{(m)} = 1$, or $\boldsymbol{p}_k^{(m)}(\xi) = (\xi, 1-\xi)$ and $\mathrm{dir}_k^{(m)} = -1$. If $\mathrm{dir}_k^{(m)} = 1$, then equalities (23) simplify to
$$\sum_{i=0}^{d} c_{i,d-i}^{(m,\ell)} B_i^d(\xi) = \theta_k(1-\xi), \quad d\sum_{i=0}^{d-1}\left(c_{i,d-i}^{(m,\ell)} + c_{i+1,d-i-1}^{(m,\ell)} - 2c_{i,d-i-1}^{(m,\ell)}\right) B_i^{d-1}(\xi) = \eta_k^{(m)}(1-\xi). \tag{24a}$$
If $\mathrm{dir}_k^{(m)} = -1$, then (23) equals
$$\sum_{i=0}^{d} c_{i,d-i}^{(m,\ell)} B_i^d(\xi) = \theta_k(\xi), \quad d\sum_{i=0}^{d-1}\left(c_{i,d-i}^{(m,\ell)} + c_{i+1,d-i-1}^{(m,\ell)} - 2c_{i,d-i-1}^{(m,\ell)}\right) B_i^{d-1}(\xi) = -\eta_k^{(m)}(\xi). \tag{24b}$$
The equalities in (24) relate the spline coefficients to the trace and directional derivative associated with the edge e_k. Moreover, they reveal the connection between the coefficients in the vertex and edge group. We see that the coefficients $c_{d,0}^{(m,\ell)}$, $c_{d-1,1}^{(m,\ell)}$ and $c_{0,d}^{(m,\ell)}$, $c_{1,d-1}^{(m,\ell)}$ from the vertex group uniquely define the boundary values and first order derivatives of the trace, *i.e.*, the values $\theta_k(0)$, $\theta_k'(0)$ and $\theta_k(1)$, $\theta_k'(1)$. Similarly, the coefficients $c_{d-1,0}^{(m,\ell)}$ and $c_{0,d-1}^{(m,\ell)}$ from the vertex group uniquely define the boundary values $\eta_k^{(m)}(0)$ and $\eta_k^{(m)}(1)$, which is equivalent to assigning the values $\omega_k(0)$ and $\omega_k(1)$. From this we conclude that there are $N_k^e = N_{k,1}^e + N_{k,2}^e + N_{k,3}^e$ degrees of freedom associated with e_k, where
$$N_{k,1}^e = |\mathbf{par}_{k,1}^e| - 4, \quad N_{k,2}^e = |\mathbf{par}_{k,2}^e| - 2, \quad N_{k,3}^e = |\mathbf{par}_{k,3}^e|.$$
Then, $N_k^e = 2d - 7 + \chi_k$, $\chi_k \in \{0,1,2\}$. Note also that $N_{k,1}^e \geq d-4$, $N_{k,2}^e \geq d-4$, and $N_{k,3}^e \in \{0,1\}$, as explained in Section 2.3 and implemented in Algorithm 2.

The coefficients in the triangle group are constrained by the super-smoothness condition $\varphi^{(m)} \in C^{d-1}(\boldsymbol{V}_{\mathrm{ct}}^{(m)})$. Since $\boldsymbol{F}_\ell^{(m)}$, $\ell = 1,2,3$, are affine reparametrizations of $\boldsymbol{F}^{(m)}$, this is equivalent to the super-smoothness condition $f^{(m)} \in C^{d-1}(\boldsymbol{v}_{\mathrm{ct}})$, which is satisfied if and only if the sets of coefficients
$$\left\{c_{r,l}^{(m,\ell)} \;:\; (r,l) \in \mathbb{I}_d,\ r+l < d\right\}, \quad \ell = 1,2,3,$$
define polynomials that can be obtained by subdividing the same polynomial $\hat{f}^{(m)} \in \mathbb{P}_{d-1}^2$.

Suppose
$$\hat{f}^{(m)}(u,v) = \sum_{(r,l)\in\mathbb{I}_{d-1}} b_{r,l}^{(m)} B_{r,l}^{d-1}(u,v). \tag{25}$$
Then the subdivision rules expressed with the help of Algorithm 1 imply that, for every $(r,l) \in \mathbb{I}_d$ such that $r+l<d$, it holds
$$c_{r,l}^{(m,1)} = \mathtt{DeCast}\left(\left\{b_{r',l'}^{(m)},\ (r',l') \in \mathbb{I}_{d-1}\right\}, \left\{(1,0)^{\langle r\rangle}, (0,1)^{\langle l\rangle}, \boldsymbol{v}_{\mathrm{ct}}^{\langle d-1-r-l\rangle}\right\}\right),$$

$$c^{(m,2)}_{r,l} = \texttt{DeCast}\left(\left\{b^{(m)}_{r',l'},\ (r',l') \in \mathbb{I}_{d-1}\right\}, \left\{(0,1)^{\langle r\rangle}, (0,0)^{\langle l\rangle}, \boldsymbol{v}_{\mathrm{ct}}^{\langle d-1-r-l\rangle}\right\}\right),$$
$$c^{(m,3)}_{r,l} = \texttt{DeCast}\left(\left\{b^{(m)}_{r',l'},\ (r',l') \in \mathbb{I}_{d-1}\right\}, \left\{(0,0)^{\langle r\rangle}, (1,0)^{\langle l\rangle}, \boldsymbol{v}_{\mathrm{ct}}^{\langle d-1-r-l\rangle}\right\}\right). \tag{26}$$

This procedure is schematically depicted in Fig. 4. Note that only $\binom{d-2}{2}$ coefficients of $\hat{f}^{(m)}$ are completely free. These are the coefficients $b^{(m)}_{r,l}$, $r = 1, 2, \dots, d-2$, $l = 1, 2, \dots, d-2-r$, which are in Fig. 4 depicted in light green color. The remaining coefficients are determined by the coefficients corresponding to the vertex and edge group as

$$b^{(m)}_{d-1-r,r} = c^{(m,1)}_{d-1-r,r}, \quad b^{(m)}_{0,d-1-r} = c^{(m,2)}_{d-1-r,r}, \quad b^{(m)}_{r,0} = c^{(m,3)}_{d-1-r,r}, \quad r = 0, 1, \dots, d-1. \tag{27}$$

The analysis of the coefficients in the vertex, edge, and triangle group leads to the following conclusion.

Theorem 1. *Let $\mathcal{T}$ be a quadratic triangulation with the vertex set $\mathcal{V}$ and the edge set $\mathcal{E}$, and let $\mathcal{T}_{\mathrm{CT}}$ be the quadratic triangulation obtained by applying the Clough–Tocher split to $\mathcal{T}$. Moreover, let $d \in \mathbb{N}$, $d \geq 4$. Then,*

$$\dim\left(\mathbb{S}_d(\mathcal{T}_{\mathrm{CT}})\right) = 3|\mathcal{V}| + \sum_{k=1}^{|\mathcal{E}|} N^e_k + \binom{d-2}{2}|\mathcal{T}|.$$

3.3. Spline construction

Following the investigation of degrees of freedom in Section 3.2, let us now propose a way to construct a spline $\varphi \in \mathbb{S}_d(\mathcal{T}_{\mathrm{CT}})$ by prescribing a set of values that on each triangle $T^{(m)} \in \mathcal{T}_{\mathrm{CT}}$ uniquely determine the coefficients in (18).

Let $\boldsymbol{V}_i \in \mathcal{V}$, and let the three degrees of freedom of φ associated with $\boldsymbol{V}_i$ be denoted by $\gamma^v_{i,1}, \gamma^v_{i,2}, \gamma^v_{i,3} \in \mathbb{R}$. They can be identified by setting the interpolation conditions

$$\varphi(\boldsymbol{V}_i) = \gamma^v_{i,1}, \quad D_x\varphi(\boldsymbol{V}_i) = \gamma^v_{i,2}, \quad D_y\varphi(\boldsymbol{V}_i) = \gamma^v_{i,3}. \tag{28}$$

To compute the coefficients from this C^1 interpolation data we first need to transform the data to the parameter domain. Let $T^{(m)} \in \mathcal{T}$ be a quadratic triangle with a vertex at $\boldsymbol{V}_i$, and let $\ell \in \{1,2,3\}$ be such that $\boldsymbol{V}_i = \left[\boldsymbol{F}^{(m)}\right]_\ell = \left[\boldsymbol{F}^{(m)}_\ell\right]_1$. Note that the second equality is due to the way we split $T^{(m)}$. Moreover, let $J\boldsymbol{F}^{(m)}_\ell$ be the Jacobian matrix of the quadratic mapping $\boldsymbol{F}^{(m)}_\ell$. Then the transformed interpolation data on $T^{(m)}_\ell$ is given by

$$f^{(m)}_\ell(1,0) = \varphi(\boldsymbol{V}_i), \quad \nabla f^{(m)}_\ell(1,0) = \left(D_x\varphi(\boldsymbol{V}_i), D_y\varphi(\boldsymbol{V}_i)\right) \cdot J\boldsymbol{F}^{(m)}_\ell(1,0).$$

Let

$$\delta^{(m)}_\ell = \gamma^v_{i,1}, \quad \left(\delta^{(m,\ell)}_{1,u}, \delta^{(m,\ell)}_{1,v}\right) = \left(\gamma^v_{i,2}, \gamma^v_{i,3}\right) \cdot J\boldsymbol{F}^{(m)}_\ell(1,0).$$

This implies

$$c^{(m,\ell)}_{d,0} = \delta^{(m)}_\ell, \quad d\left(c^{(m,\ell)}_{d,0} - c^{(m,\ell)}_{d-1,0}, c^{(m,\ell)}_{d-1,1} - c^{(m,\ell)}_{d-1,0}\right) = \left(\delta^{(m,\ell)}_{1,u}, \delta^{(m,\ell)}_{1,v}\right)$$

and uniquely determines

$$c^{(m,\ell)}_{d,0} = \delta^{(m)}_\ell, \quad c^{(m,\ell)}_{d-1,0} = \delta^{(m)}_\ell - \frac{1}{d}\delta^{(m,\ell)}_{1,u}, \quad c^{(m,\ell)}_{d-1,1} = \delta^{(m)}_\ell - \frac{1}{d}\left(\delta^{(m,\ell)}_{1,u} - \delta^{(m,\ell)}_{1,v}\right).$$

Similarly, because $\left[\boldsymbol{F}^{(m)}_\ell\right]_1 = \left[\boldsymbol{F}^{(m)}_{\ell^-}\right]_2$, where $\ell^- = \mathrm{mod}(\ell+1,3)+1$ is the index before ℓ in the cyclic notation, it follows that

$$c^{(m,\ell^-)}_{0,d} = \delta^{(m)}_\ell, \quad c^{(m,\ell^-)}_{0,d-1} = \delta^{(m)}_\ell - \frac{1}{d}\delta^{(m,\ell^-)}_{2,v}, \quad c^{(m,\ell^-)}_{1,d-1} = \delta^{(m)}_\ell + \frac{1}{d}\left(\delta^{(m,\ell^-)}_{2,u} - \delta^{(m,\ell^-)}_{2,v}\right),$$

where

$$\left(\delta^{(m,\ell^-)}_{2,u}, \delta^{(m,\ell^-)}_{2,v}\right) = \left(\gamma^v_{i,2}, \gamma^v_{i,3}\right) \cdot J\boldsymbol{F}^{(m)}_{\ell^-}(0,1).$$

This way the coefficients (19) in the vertex group are uniquely determined.

Let $e_k \in \mathcal{E}$, and let the N^e_k degrees of freedom of φ associated with e_k be denoted by $\gamma^e_{k,r,0} \in \mathbb{R}$, $r = 1, 2, \dots, N^e_{k,1}$, and $\gamma^e_{k,r,1} \in \mathbb{R}$, $r = 1, 2, \dots, N^e_{k,2} + N^e_{k,3}$. They can be identified by setting the interpolation conditions as follows.

- Let $\xi_{k,r,0}$, $r = 0, 1, \dots, N^e_{k,1}$, be some distinct parameters from the interval $(0,1)$, and for each $\xi_{k,r,0}$ let $\boldsymbol{V}^e_{k,r,0} = \boldsymbol{F}^{(m)}(\boldsymbol{p}^{(m)}_k(\xi_{k,r,0}))$ be the associated point on e_k. We prescribe

$$\varphi(\boldsymbol{V}^e_{k,r,0}) = \theta_k(\xi_{k,r,0}) = \gamma^e_{k,r,0}, \quad r = 1, 2, \dots, N^e_{k,1}. \tag{29a}$$

- Let $\xi_{k,r,1}$, $r = 0, 1, \dots, N^e_{k,2} + N^e_{k,3}$, be some distinct parameters from the interval $(0,1)$, and for each $\xi_{k,r,1}$ let $\boldsymbol{V}^e_{k,r,1} = \boldsymbol{F}^{(m)}(\boldsymbol{p}^{(m)}_k(\xi_{k,r,1}))$ be the associated point on e_k. We prescribe

$$D_{\boldsymbol{n}_k(\xi_{k,r,1})}\varphi(\boldsymbol{V}^e_{k,r,1}) = \frac{\omega_k(\xi_{k,r,1})}{q_k(\xi_{k,r,1})} = \gamma^e_{k,r,1}, \quad r = 1, 2, \dots, N^e_{k,2}, \tag{29b}$$

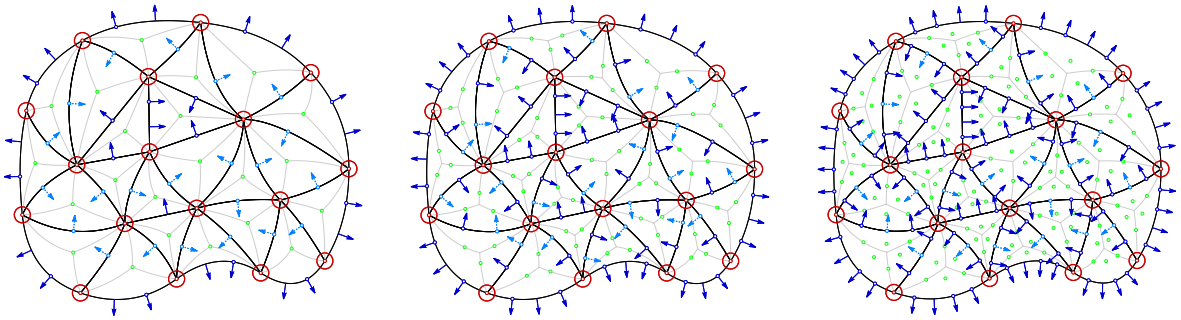

Fig. 5. A schematic representation of the interpolation problem described in Theorem 2 over the quadratic triangulation in Fig. 3 (left) for degrees $d = 4$ (left), $d = 5$ (center), and $d = 6$ (right). The red points and circles symbolize the interpolation of values and first order derivative values at the vertices, *i.e.* the interpolation conditions (28). The interpolation conditions (29) related to the edges are depicted in blue color. Notice that they are not the same for every edge as they depend on the geometry of the attached quadratic triangles. The conditions (29a) are denoted by the blue points, the conditions (29b) by the blue arrows and the condition (29c) by the light blue points with dashed arrows. The positions of these points and arrows are computed using Algorithm 4. The interpolation points corresponding to the conditions (30) are shown in green.

and, additionally, if $N^e_{k,3} = 1$,

$$D_{\boldsymbol{n}_k(\xi_{k,r,1})}\varphi(\boldsymbol{V}^e_{k,r,1}) + D_{\boldsymbol{t}_k(\xi^e_{k,r,1})}\varphi(\boldsymbol{V}^e_{k,r,1}) = \frac{\omega_k(\xi_{k,r,1})}{q_k(\xi_{k,r,1})} + \theta'_k(\xi_{k,r,1}) = \gamma^e_{k,r,1}, \quad r = N^e_{k,2} + N^e_{k,3}. \tag{29c}$$

A particular choice of the parameters $\xi_{k,r,0}$ and $\xi_{k,r,1}$ is provided by Algorithm 4, where the parameters are selected equidistantly and with the aim to take as many parameters $\xi_{k,r,0}$ and $\xi_{k,r,1}$ as possible to be equal so that at the corresponding points on the edge the values as well as normal derivatives are interpolated. Since $N^e_{k,1} \le N^e_{k,2} \le N^e_{k,1} + 2$, there are at most two points at which only the normal derivatives and not values are interpolated. However, for the solvability of the interpolation problem, it is only necessary that $\{\xi_{k,r,0}\}_r$ are pairwise distinct and the same for $\{\xi_{k,r,1}\}_r$. More in-depth analysis on the effect of the choice of these parameters on the interpolating spline is beyond the scope of this paper.

Consider a triangle $T^{(m)}_{\ell} \in \mathcal{T}_{\mathrm{CT}}$ with the edge e_k. Together with the values $\theta_k(0)$, $\theta'_k(0)$, $\theta_k(1)$, $\theta'_k(1)$, $\omega_k(0)$, $w_k(1)$, which are fixed by the degrees of freedom associated with the endpoints of e_k, the interpolation conditions (29) uniquely determine the univariate polynomials θ_k and ω_k, and hence by (24) the coefficients (20) in the edge group.

Let $T^{(m)} \in \mathcal{T}$. The $\binom{d-2}{2}$ degrees of freedom of φ associated with $T^{(m)}$ can be identified by a subset of coefficients of the polynomial in (25). On the other hand, we can again describe these degrees of freedom by interpolation. Let $\gamma^t_{m,i,j} \in \mathbb{R}$, $i = 1, 2, \dots, d-2$, $j = 1, 2, \dots, d-2-i$, be given values, and let us prescribe that

$$\varphi(\boldsymbol{V}^t_{m,r,l}) = \gamma^t_{m,r,l}, \quad r = 1, 2, \dots, d-2, \ l = 1, 2, \dots, d-2-r, \tag{30}$$

where $\boldsymbol{V}^t_{m,r,l} = \boldsymbol{F}^{(m)}(\frac{r}{d-1}, \frac{l}{d-1})$. Together with the interpolation conditions (28) corresponding to the vertices of $T^{(m)}$ and the interpolation conditions (29) corresponding to the edges of $T^{(m)}$, the conditions in (30) uniquely determine the coefficients (21) in the triangle group.

The above discussion can be summarized to the following result.

Theorem 2. *Let $\mathcal{T}$ be a quadratic triangulation with the vertex set $\mathcal{V}$ and the edge set $\mathcal{E}$, and let $\mathcal{T}_{\mathrm{CT}}$ be the quadratic triangulation obtained by applying the Clough–Tocher split to $\mathcal{T}$. Moreover, let $d \in \mathbb{N}$, $d \ge 4$. Suppose that*

- *three values $\gamma^v_{i,r} \in \mathbb{R}$, $r = 1, 2, 3$, for every $\boldsymbol{V}_i \in \mathcal{V}$ are given;*
- *N^e_k values $\gamma^e_{k,r,0} \in \mathbb{R}$, $r = 1, 2, \dots, N^e_{k,1}$, and $\gamma^e_{k,r,1} \in \mathbb{R}$, $r = 1, 2, \dots, N^e_{k,2} + N^e_{k,3}$, for every $e_k \in \mathcal{E}$ are given;*
- *$\binom{d-2}{2}$ values $\gamma^t_{m,r,l} \in \mathbb{R}$, $r = 1, 2, \dots, d-2$, $l = 1, 2, \dots, d-2-r$, for every $T^{(m)} \in \mathcal{T}$ are given.*

Then, there exists a unique spline $\varphi \in \mathbb{S}_d(\mathcal{T}_{\mathrm{CT}})$ satisfying the interpolation conditions (28), (29), (30).

Fig. 5 shows a schematic representation of the interpolation problem described in Theorem 2 over a quadratic triangulation for degrees $d = 4, 5, 6$.

3.4. Basis functions

An important ingredient of various classical methods in numerical analysis is the representation of an approximation in terms of basis functions. In what follows we demonstrate that the spline space $\mathbb{S}_d(\mathcal{T}_{\mathrm{CT}})$ can be equipped with locally supported basis functions that naturally emerge from the discussion in Section 3.3.

Following Theorem 1, let us introduce three types of basis functions:

- the basis functions $B^v_{i,r}$, $r = 1, 2, 3$, for every vertex $\boldsymbol{V}_i \in \mathcal{V}$;
- the basis functions $B^e_{k,r}$, $r = 1, 2, \dots, N^e_k$, for every edge $e_k \in \mathcal{E}$;
- the basis functions $B^t_{m,r,l}$, $r = 1, 2, \dots, d-2$, $l = 1, 2, \dots, d-2-r$, for every $T^{(m)} \in \mathcal{T}$.

To define these basis functions we use the interpolation conditions in (28) and (29) and a subset of coefficients of the polynomial (25). We follow the concepts behind the scaled nodal basis functions in the theory of finite elements.

For a vertex $\boldsymbol{V}_i \in \mathcal{V}$, let h^v_i denote the length of the longest line connecting the vertex $\boldsymbol{V}_i$ to a vertex from $\mathcal{V}$ that is connected to $\boldsymbol{V}_i$ with an edge. Similarly, for an edge $e_k \in \mathcal{E}$, let h^e_k denote the length of the line connecting the endpoints of e_k. For a vertex $\boldsymbol{V}_{i^*} \in \mathcal{V}$ and $r^* \in \{1, 2, 3\}$, let $B^v_{i^*,r^*}$ be defined by

- the interpolation conditions in (28) with

$$\gamma^v_{i,1} = \begin{cases} 1 & \text{if } (i^*, r^*) = (i, 1), \\ 0 & \text{otherwise,} \end{cases} \qquad \gamma^v_{i,2} = \begin{cases} \frac{1}{h^v_{i^*}} & \text{if } (i^*, r^*) = (i, 2), \\ 0 & \text{otherwise,} \end{cases} \qquad \gamma^v_{i,3} = \begin{cases} \frac{1}{h^v_{i^*}} & \text{if } (i^*, r^*) = (i, 3), \\ 0 & \text{otherwise,} \end{cases}$$

  for $i = 1, 2, \dots, |\mathcal{V}|$;
- the interpolation conditions in (29) with

$$\gamma^e_{k,r,0} = 0, \quad r = 1, 2, \dots, N^e_k, \qquad \gamma^e_{k,r,1} = 0, \quad r = 1, 2, \dots, N^e_{k,2} + N^e_{k,3}$$

  for $k = 1, 2, \dots, |\mathcal{E}|$;
- the coefficients

$$b^{(m)}_{r,l} = 0, \quad r = 1, 2, \dots, d-2, \ l = 1, 2, \dots, d-2-r,$$

  for $m = 1, 2, \dots, |\mathcal{T}|$.

For an edge $e_{k^*} \in \mathcal{E}$ and $r^* \in \{1, 2, \dots, N^e_k\}$, let $B^e_{k^*,r^*}$ be defined by

- the interpolation conditions in (28) with

$$\gamma^v_{i,r} = 0, \quad r = 1, 2, 3,$$

  for $i = 1, 2, \dots, |\mathcal{V}|$;
- the interpolation conditions in (29) with

$$\gamma^e_{k,r,0} = \begin{cases} 1 & \text{if } (k^*, r^*) = (k, r), \\ 0 & \text{otherwise,} \end{cases} \qquad r = 1, 2, \dots, N^e_{k,1},$$

$$\gamma^e_{k,r,1} = \begin{cases} \frac{1}{h^e_k} & \text{if } (k^*, r^*) = (k, N^e_{k,1} + r), \\ 0 & \text{otherwise,} \end{cases} \qquad r = 1, 2, \dots, N^e_{k,2} + N^e_{k,3},$$

  for $k = 1, 2, \dots, |\mathcal{E}|$;
- the coefficients

$$b^{(m)}_{r,l} = 0, \quad r = 1, 2, \dots, d-2, \ l = 1, 2, \dots, d-2-r,$$

  for $m = 1, 2, \dots, |\mathcal{T}|$.

For a triangle $T^{(m^*)} \in \mathcal{T}$ and (r^*, l^*) such that $(r^* - 1, l^* - 1) \in \mathbb{I}_{d-4}$, let $B^t_{m^*,r^*,l^*}$ be defined by

- the interpolation conditions in (28) with

$$\gamma^v_{i,r} = 0, \quad r = 1, 2, 3,$$

  for $i = 1, 2, \dots, |\mathcal{V}|$;
- the interpolation conditions in (29) with

$$\gamma^e_{k,r,0} = 0, \quad r = 1, 2, \dots, N^e_k, \qquad \gamma^e_{k,r,1} = 0, \quad r = 1, 2, \dots, N^e_{k,2} + N^e_{k,3}$$

  for $k = 1, 2, \dots, |\mathcal{E}|$;
- the coefficients

$$b^{(m)}_{r,l} = \begin{cases} 1 & \text{if } (m^*, r^*, l^*) = (m, r, l), \\ 0 & \text{otherwise,} \end{cases} \qquad r = 1, 2, \dots, d-2, \ l = 1, 2, \dots, d-2-r,$$

  for $m = 1, 2, \dots, |\mathcal{T}|$.

Examples of basis functions of degree 5 associated with a vertex, an edge, and a triangle are shown in Figs. 6, 7, and 8, respectively.

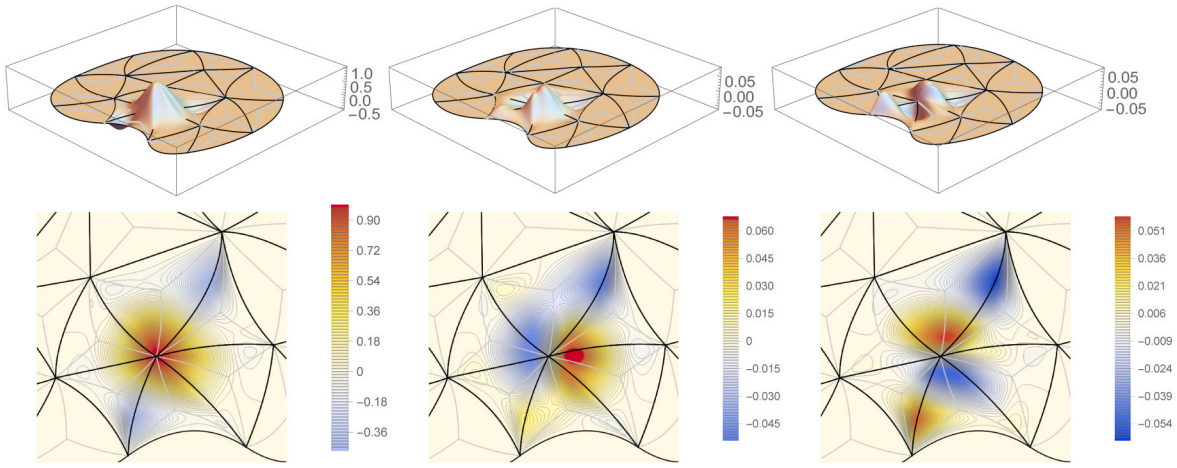

Fig. 6. The three basis functions of degree 5 associated with a vertex of a quadratic triangulation. The pictures above show the graphs and the pictures below show excerpts of the contour plots of the basis functions.

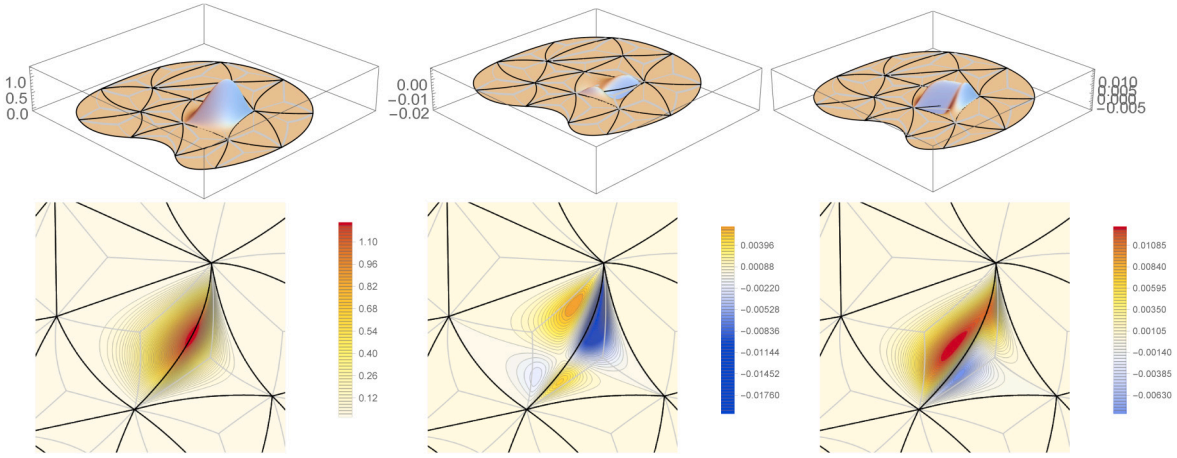

Fig. 7. The three basis functions of degree 5 associated with a generic edge of a quadratic triangulation. The pictures above show the graphs and the pictures below show excerpts of the contour plots of the basis functions.

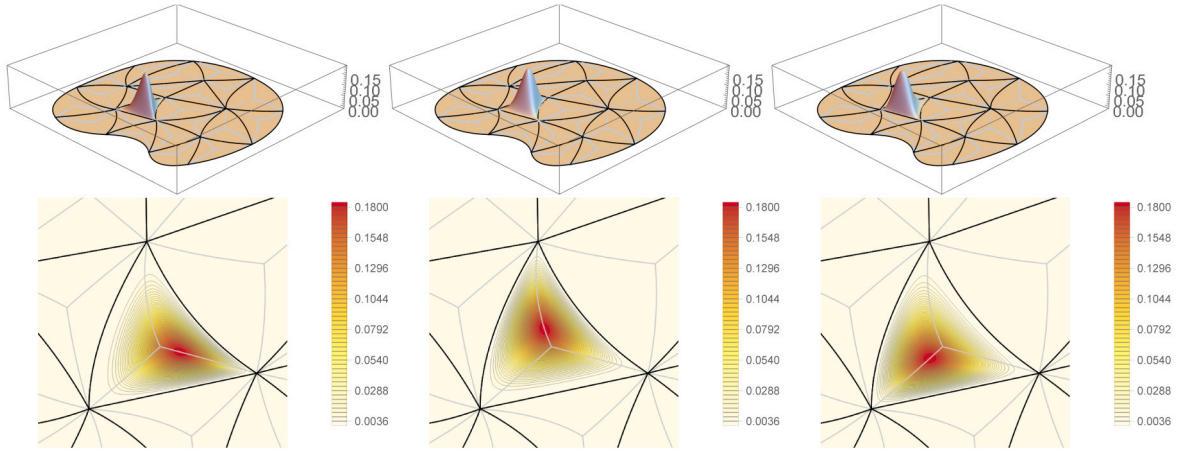

Fig. 8. The three basis functions of degree 5 associated with a triangle of a quadratic triangulation. The pictures above show the graphs and the pictures below show excerpts of the contour plots of the basis functions.

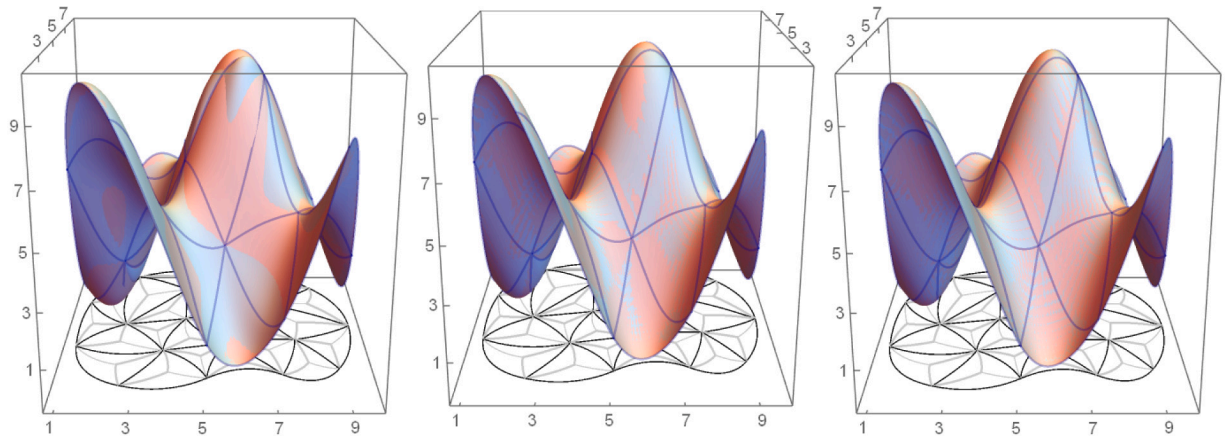

Fig. 9. Graphs of the interpolants from Example 1 (in light blue color) of degrees 4 (left), 5 (center), and 6 (right) plotted together with the interpolated function (in orange color).

Table 1
The interpolation errors corresponding to Example 1 (left), Example 3 (center), and Example 4 (right).

d	NDOF	Error	d	NDOF	Error	d	NDOF	Error
4	118	$5.22 \cdot 10^{-1}$	4	371	$2.01 \cdot 10^{-1}$	4	449	$4.43 \cdot 10^{-2}$
5	197	$1.22 \cdot 10^{-1}$	5	616	$8.73 \cdot 10^{-3}$	5	694	$4.40 \cdot 10^{-3}$
6	277	$3.12 \cdot 10^{-2}$	6	862	$5.10 \cdot 10^{-3}$	6	940	$4.31 \cdot 10^{-4}$
7	358	$1.54 \cdot 10^{-3}$	7	1109	$8.60 \cdot 10^{-4}$	7	1187	$3.77 \cdot 10^{-5}$
8	440	$6.45 \cdot 10^{-4}$	8	1357	$1.98 \cdot 10^{-5}$	8	1435	$4.71 \cdot 10^{-6}$
9	523	$1.26 \cdot 10^{-4}$	9	1606	$8.22 \cdot 10^{-6}$	9	1684	$6.69 \cdot 10^{-7}$
10	607	$7.30 \cdot 10^{-6}$	10	1856	$1.11 \cdot 10^{-6}$	10	1934	$5.04 \cdot 10^{-8}$

3.5. Numerical examples

Finally, we provide some numerical examples of splines from the space $\mathbb{S}_d\left(\mathcal{T}_{\mathrm{CT}}\right)$ obtained by interpolation and compare how the interpolation error behaves in dependence of the degree d.

Suppose $\psi : \Omega \to \mathbb{R}$ is a function we wish to interpolate, and let us assume that ψ is differentiable. Let $d \in \mathbb{N}$, $d \geq 4$. For every $\boldsymbol{V}_i \in \mathcal{V}$, let

$$\gamma^v_{i,1} = \psi(\boldsymbol{V}_i), \quad \gamma^v_{i,2} = D_x\psi(\boldsymbol{V}_i), \quad \gamma^v_{i,3} = D_y\psi(\boldsymbol{V}_i).$$

Moreover, for every $e_k \in \mathcal{E}$, let

$$\gamma^e_{k,r,0} = \psi(\boldsymbol{V}^e_{k,r,0}), \quad r = 1, 2, \ldots, N^e_{k,1}, \qquad \gamma^e_{k,r,1} = D_{\boldsymbol{n}_k(\xi_{k,r,1})}\psi(\boldsymbol{V}^e_{k,r,1}), \quad r = 1, 2, \ldots, N^e_{k,2},$$

and, if $N^e_{k,3} = 1$,

$$\gamma^e_{k,r,1} = D_{\boldsymbol{n}_k(\xi_{k,r,1})}\psi(\boldsymbol{V}^e_{k,r,1}) + D_{\boldsymbol{t}_k(\xi^e_{k,r,1})}\psi(\boldsymbol{V}^e_{k,r,1}), \quad r = N^e_{k,2} + N^e_{k,3}.$$

Finally, for every $T^{(m)} \in \mathcal{T}$, let

$$\gamma^t_{m,r,l} = \psi(\boldsymbol{V}^t_{m,r,l}), \quad r = 1, 2, \ldots, d-2, \; l = 1, 2, \ldots, d-2-r.$$

By Theorem 2 these values uniquely determine a spline from $\mathbb{S}_d(\mathcal{T}_{\mathrm{CT}})$ that we denote by $\mathcal{I}_d\psi$. In the following examples we examine the maximal absolute error $|\psi - \mathcal{I}_d\psi|$, which is estimated on a dense set of points selected from Ω, for different choices of Ω and ψ.

Example 1. Let Ω and its associated partition be as shown in Fig. 3 (left), and let

$$\psi(x, y) = 5\left(\sin(\tfrac{\pi}{4}x)\sin(\tfrac{\pi}{4}y) + 1\right). \tag{31}$$

Fig. 9 shows graphs of the interpolants of degrees 4, 5, and 6. The interpolation results for degrees $4, 5, \ldots, 10$ are provided in Table 1 (left) and graphically displayed in Fig. 10.

Example 1 clearly shows that the interpolation error decreases with the increasing degree. In the next example we investigate the polynomial reproduction properties. As the geometry mappings are quadratic, it is expected that an interpolating spline of degree d reproduces polynomials of total degree at most $\lfloor \frac{d}{2} \rfloor$.

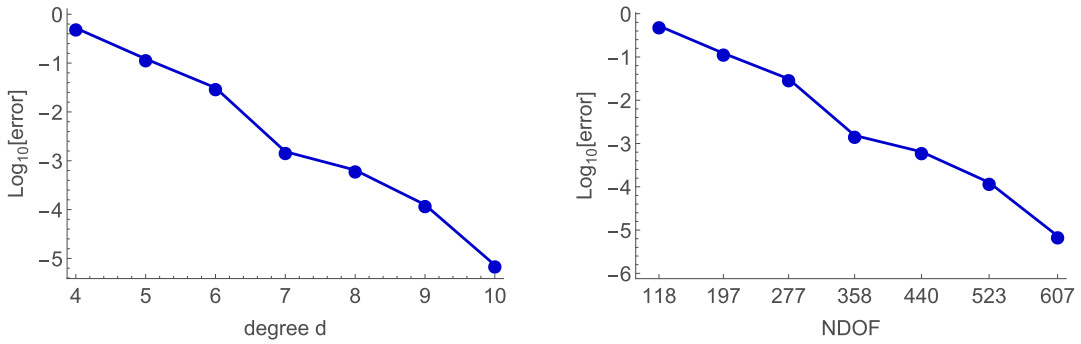

Fig. 10. Graphical display of the interpolation errors from Example 1 with respect to degree (left) and NDOF (right).

Table 2
Interpolation errors corresponding to Example 2. A value in the upper row represents the spline degree d followed by the number of degrees of freedom in bracket. A value in the left column represents the polynomial degree δ. The value in table corresponding to a pair (δ, d) is the interpolation error obtained by interpolating the polynomial ψ of degree δ defined in (32) with the spline $\mathcal{I}_d\psi$.

	4 (118)	5 (197)	6 (277)	7 (358)	8 (440)	9 (523)	10 (607)
2	0	0	0	0	0	0	0
3	$3.80 \cdot 10^{-3}$	$1.26 \cdot 10^{-4}$	0	0	0	0	0
4	$3.80 \cdot 10^{-3}$	$3.14 \cdot 10^{-4}$	$1.60 \cdot 10^{-5}$	$5.64 \cdot 10^{-7}$	0	0	0
5	$2.70 \cdot 10^{-3}$	$3.11 \cdot 10^{-4}$	$2.98 \cdot 10^{-5}$	$1.61 \cdot 10^{-6}$	$5.04 \cdot 10^{-8}$	$2.76 \cdot 10^{-9}$	0
6	$2.99 \cdot 10^{-3}$	$3.27 \cdot 10^{-4}$	$3.12 \cdot 10^{-5}$	$2.75 \cdot 10^{-6}$	$1.56 \cdot 10^{-7}$	$6.26 \cdot 10^{-9}$	$2.07 \cdot 10^{-10}$

Table 3
The errors when interpolating the function (31) using degrees $d = 4$, $d = 5$, and $d = 6$ with splines over triangulations from Fig. 13 (partition A and B) on different levels of refinement together with the estimated decay exponent ρ, the number of degrees of freedom (NDOF) and the mesh size h.

partition A										
		$d = 4$			$d = 5$			$d = 6$		
Level	h	NDOF	Error	ρ	NDOF	Error	ρ	NDOF	Error	ρ
0	2.32	54	$1.05 \cdot 10^{-1}$	/	87	$1.49 \cdot 10^{-2}$	/	121	$1.04 \cdot 10^{-3}$	/
1	1.26	198	$7.90 \cdot 10^{-3}$	4.26	309	$6.76 \cdot 10^{-4}$	5.09	421	$2.00 \cdot 10^{-5}$	6.51
2	0.73	774	$5.97 \cdot 10^{-4}$	4.75	1185	$2.18 \cdot 10^{-5}$	6.31	1597	$3.40 \cdot 10^{-7}$	7.49
3	0.39	3078	$4.44 \cdot 10^{-5}$	4.16	4665	$6.97 \cdot 10^{-7}$	5.51	6253	$5.36 \cdot 10^{-9}$	6.65
partition B										
Level	h	NDOF	Error	ρ	NDOF	Error	ρ	NDOF	Error	ρ
0	2.10	72	$1.63 \cdot 10^{-2}$	/	105	$1.42 \cdot 10^{-3}$	/	139	$1.21 \cdot 10^{-4}$	/
1	1.05	234	$7.20 \cdot 10^{-4}$	4.50	345	$3.29 \cdot 10^{-5}$	5.43	457	$1.32 \cdot 10^{-6}$	6.52
2	0.526	846	$2.31 \cdot 10^{-5}$	4.96	1257	$5.33 \cdot 10^{-7}$	5.95	1669	$1.05 \cdot 10^{-8}$	6.97
3	0.263	3222	$7.24 \cdot 10^{-7}$	4.99	4809	$8.37 \cdot 10^{-9}$	5.99	6397	$8.25 \cdot 10^{-11}$	6.99

Example 2. Let Ω and its associated partition be as shown in Fig. 3 (left), and let ψ be a polynomial of a chosen total degree $\delta \geq 2$ given by

$$\psi(x, y) = \frac{4}{20^{\delta-1}}(x-5)(y-4)(x+y)^{\delta-2} + 2. \tag{32}$$

The interpolation results for $\delta = 2, 3, 4, 5$ and $d = 4, 5, \ldots, 10$ are provided in Table 2.

Examples 3 and 4 are similar to Example 1 but performed on a non-convex domain (center and right picture of Fig. 3) partitioned so that, firstly, all edges are curved, and secondly, all interior edges are uniformly parametrized straight lines.

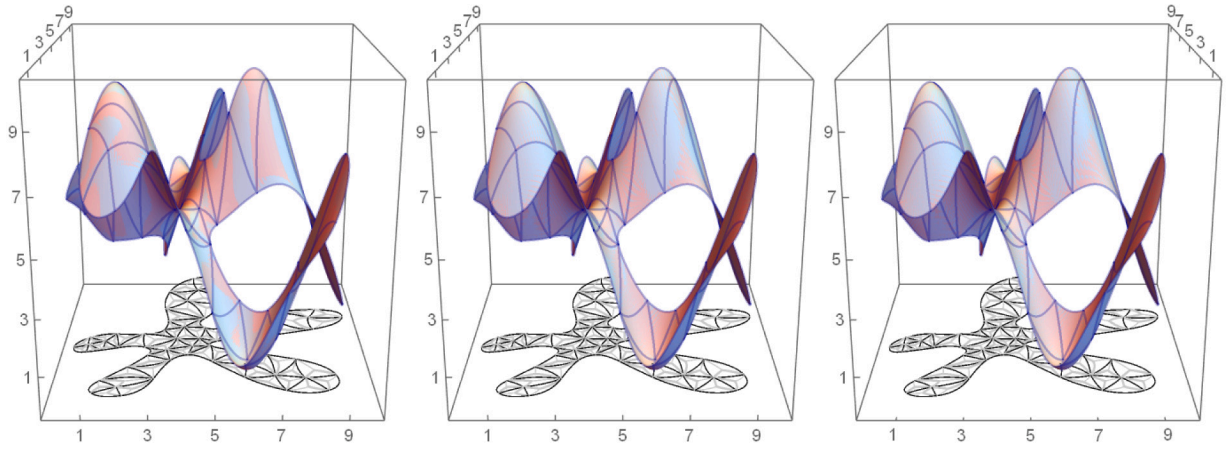

Fig. 11. Graphs of the interpolants from Example 3 (in light blue color) of degrees 4 (left), 5 (center), and 6 (right) plotted together with the interpolated function (in orange color).

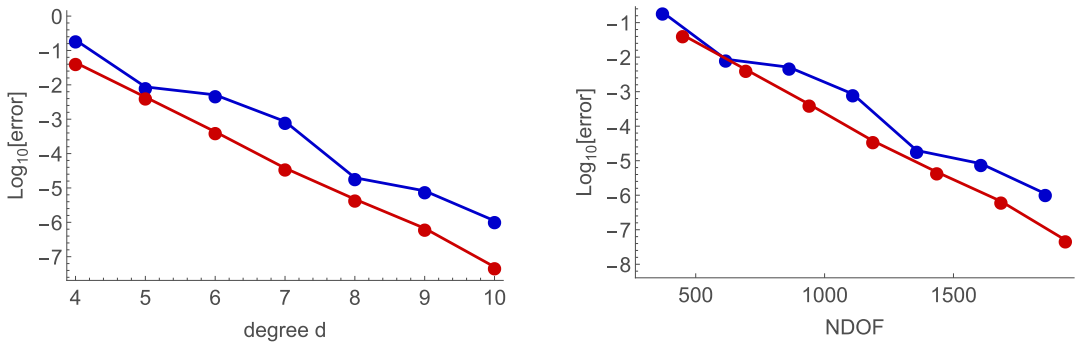

Fig. 12. Graphical display of the interpolation errors from Example 3 (blue color) and Example 4 (red color) with respect to degree (left) and NDOF (right).

Example 3. Let Ω and its associated partition be as shown in Fig. 3 (center), and let ψ be given by (31). Fig. 11 shows graphs of the interpolants of degrees 4, 5, and 6. The interpolation results for degrees $4, 5, \ldots, 10$ are provided in Table 1 (center) and graphically displayed in Fig. 12.

Example 4. Let Ω and its associated partition be as shown in Fig. 3 (right), and let ψ be given by (31). The interpolation results are provided in Table 1 (right) and graphically displayed in Fig. 12.

Fig. 12 indicates that splines on a linearly partitioned domain ensure better accuracy, but the trend of the interpolation error is the same in both examples.

In the last example we demonstrate the behavior of the interpolation error in terms of the decreasing mesh size of the partition.

Example 5. The chosen zero-level quadratic triangulation (partition A) with Clough–Tocher split together with three levels of refinement is shown in Fig. 13 (top), and its linear counterpart (partition B) is shown in the bottom line. In more detail, the refinement of each macro quadratic triangle is done by the dyadic refinement of the domain triangle $\triangle$. The corresponding geometry mappings are computed by the subdivision of the starting–zero level geometry mappings. Therefore, for the refined triangulation, the number of degrees of freedom corresponding to the edges that lie in the interior of zero-level macro triangles is the maximal possible, *i.e.*, $2d + 1$. Namely, the neighboring geometry mappings are (because of the subdivision) C^1 continuous, thus (in the Algorithm 2) the gluing functions α_1 and α_2 have a common quadratic factor and therefore the degree of ω increases by two. Note that for such an edge we associate the free parameter μ_2 to the trace function and not to a combination of the trace and ω in order

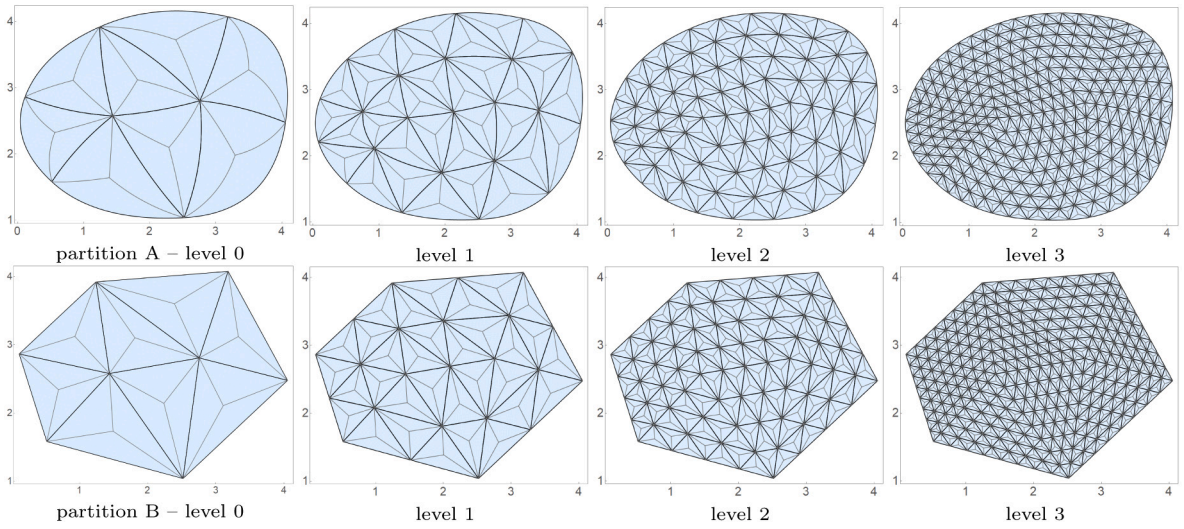

Fig. 13. Top: A quadratic triangulation (partition A) with the Clough–Tocher split (left) and its three levels of refinement. Bottom: A linear triangulation (partition B) with the Clough–Tocher split (left) and its three levels of refinement.

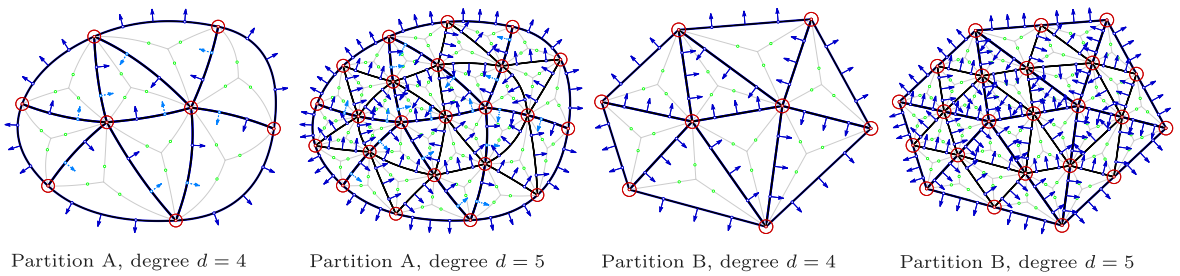

Fig. 14. Schematic representation of the interpolation conditions for degrees $d = 4$ and $d = 5$ on the zero and first refinement level for partitions A and B.

to set the same interpolation conditions as in the case of a linear triangulation (and boundary edges). This is illustrated in Fig. 14 where the interpolation conditions for degrees $d = 4$ and $d = 5$ over the zero-level and the first-level triangulations are schematically shown for the quadratic as well as for the linear triangulation.

Table 3 shows the errors when interpolating the function (31) using degrees $d = 4$, $d = 5$, and $d = 6$ over triangulations from Fig. 13 (partitions A and B). The mesh size h is taken to be the maximal length of edges of the triangulation. Note that for the partition A the value h does not decrease by the factor 2 since the edges of zero-level quadratic triangulation are not uniformly parameterized. The estimated decay exponent ρ (shown in the columns 5,8, and 11), indicates that for the quadratic triangulation the approximation order does not drop below the chosen degree d, although the geometry mappings are quadratic and up to two degrees of freedom are lost over the edges of the zero-level triangulation. For the linear triangulation (partition B), where the number of degrees of freedom is $2d + 1$ per edge, the estimated approximation order is $d + 1$ as expected. The graph of the interpolation errors (in a logarithmic scale) with respect to the level of refinement (left) and NDOF (right) for degrees 4, 5 and 6, is shown in Fig. 15 for both types of the partition. One can observe that on each refinement step the errors of interpolants of degree d over the quadratic triangulation are comparable to the errors of interpolants of degree $d + 1$ over the linear triangulation.

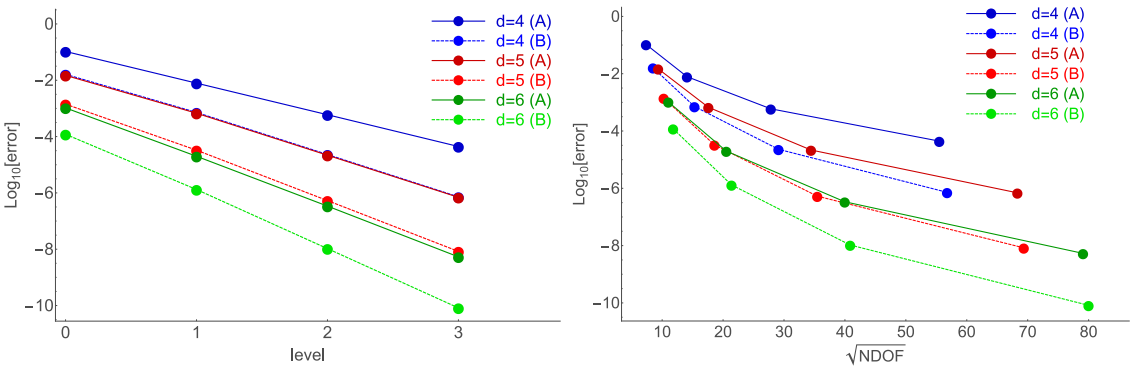

Fig. 15. Graphical display of the interpolation errors from Example 5 for the quadratic triangulation (A) and the linear triangulation (B) with respect to the level of refinement (left) and NDOF (right) for degrees 4, 5, and 6.

4. Conclusions

The paper provides a spline framework for curved domains that is considerably more flexible than the common isoparametric framework. The presented methods enable local construction of C^1 splines on partitions consisting of quadratic elements that join only continuously. This flexibility does not come without difficulties, namely the C^1 smoothness constraints across neighboring geometry elements depend heavily on their parametrization, and the number of degrees of freedom of a resulting spline can vary from one edge of the partition to the other. In particular, for the considered approach that utilizes the Clough–Tocher splitting, this phenomenon implies that the degree of the splines must be at least four.

Potentially, the proposed framework could be generalized to allow the construction of splines on a partition of a surface. Local geometry mappings with three components give rise to a quadratic triangulation in space. But to study the C^1 smoothness conditions in this setting, one obvious requirement is that the local geometry mappings form a G^1 smooth surface so that the tangent planes along the edge parametrizations are well defined. In the planar case this is inherently true as every continuous mapping is G^1 smooth. In general, however, constructing G^1 smooth quadratic surfaces is more challenging but somehow crucial since geometry mappings of higher degrees are expected to bring further complications in analysis of smoothness conditions, as well as reduction of approximation order.

CRediT authorship contribution statement

Jan Grošelj: Writing – review & editing, Writing – original draft, Methodology, Investigation, Formal analysis, Conceptualization. **Marjeta Knez:** Writing – review & editing, Writing – original draft, Validation, Software, Methodology, Investigation, Formal analysis, Conceptualization.

Acknowledgments

The work was partially supported by Javna agencija za znanstvenoraziskovalno in inovacijsko dejavnost Republike Slovenije (ARIS) in the scope of the research programs P1-0294 (J. Grošelj) and P1-0288 (M. Knez), the research grants N1–0237 and J1–3005 (M. Knez), and the project BI–AT/23–24–018.

Appendix A. Algorithms

This section contains pseudocode for the algorithms that were used in the paper with the aim to provide details on technical aspects of the computations. Algorithms 2 and 3 assume implementation in a package for symbolic computation. The naming of the variables in the algorithms follows the notation from the paper but for better readability some edge related lower indices are omitted and some triangle related upper indices are changed to lower.

Algorithm 2: Trace and directional derivative (`TrAndDer`)

Input: Geometry mappings $\boldsymbol{F}^{(\ell)} : \Delta \to T^{(\ell)}$, $\ell = 1, 2$; parametrizations $\boldsymbol{p}^{(\ell)} : [0, 1] \to e_k$; degree d

$\boldsymbol{J}_\ell(\xi) \leftarrow J\boldsymbol{F}^{(\ell)}(\boldsymbol{p}^{(\ell)}(\xi))$, $\ell = 1, 2$;

$\boldsymbol{\sigma}_\ell \leftarrow \frac{d}{d\xi}\boldsymbol{p}^{(\ell)}(\xi)|_{\xi=0}$, $\ell = 1, 2$;

$\boldsymbol{n}(\xi) \leftarrow \left(\boldsymbol{\sigma}_1 \cdot \boldsymbol{J}_1(\xi)^T\right)^\perp$;

$\beta(\xi) \leftarrow \|\boldsymbol{n}(\xi)\|$;

$\alpha_\ell(\xi) \leftarrow \|\boldsymbol{\sigma}_\ell\|^2 \det \boldsymbol{J}_\ell(\xi)$, $\ell = 1, 2$;

$\beta_\ell(\xi) \leftarrow \left\langle \left(\boldsymbol{\sigma}_\ell{}^\perp \cdot \boldsymbol{J}_\ell(\xi)^T\right)^\perp, \boldsymbol{n}(\xi) \right\rangle$, $\ell = 1, 2$;

$q(\xi) \leftarrow \gcd(\alpha_1(\xi), \alpha_2(\xi); \xi)$;

$\widetilde{\alpha}_\ell(\xi) \leftarrow \mathrm{quot}(\alpha_\ell(\xi), q(\xi); \xi)$, $\ell = 1, 2$;

$d_k \leftarrow d - 1 - \max\left\{\deg(\widetilde{\alpha}_1), \deg(\widetilde{\alpha}_2)\right\}$;

if $\deg(\beta) = 2$ **then**

  $\widehat{\alpha}_\ell(\xi) \leftarrow \mathrm{rem}(\widetilde{\alpha}_\ell(\xi), \beta(\xi); \xi)$, $\ell = 1, 2$;

  $\widehat{\beta}_\ell(\xi) \leftarrow \mathrm{rem}(\beta_\ell(\xi), \beta(\xi); \xi)$, $\ell = 1, 2$;

  $\left\{\hat{\tau}(\xi), \hat{\omega}(\xi), \left\{\mu_1, \mu_2\right\}\right\} = \mathtt{TrAndDerRem}(\widehat{\alpha}_1(\xi), \widehat{\alpha}_2(\xi), \widehat{\beta}_1(\xi), \widehat{\beta}_2(\xi), \beta(\xi))$;

  $\tau^*(\xi) \leftarrow \sum_{i=0}^{d-3} \tau_i B_i^{d-3}(\xi)$;

  $\tau(\xi) \leftarrow \beta(\xi)\tau^*(\xi) + \hat{\tau}(\xi)$;

  $\theta(\xi) \leftarrow \vartheta_0 + \int_0^\xi \tau(\xi) d\xi$;

  $\omega^*(\xi) \leftarrow \sum_{i=0}^{d_k} \omega_i B_i^{d_k}(\xi)$;

  $\omega(\xi) \leftarrow \beta(\xi)\omega^*(\xi) + \hat{\omega}(\xi)$;

  par $\leftarrow \left\{\left\{\vartheta_0, \tau_0, \ldots, \tau_{d-3}, \mu_1\right\}, \left\{\omega_0, \omega_1, \ldots, \omega_{d_k}\right\}, \left\{\mu_2\right\}\right\}$;

else

  if $\deg(\widetilde{\alpha}_1\beta_2 - \widetilde{\alpha}_1\beta_2) = \max(\deg(\widetilde{\alpha}_1), \deg(\widetilde{\alpha}_2)) + 1$ **then**

    $\theta(\xi) \leftarrow \sum_{i=0}^{d-1} \vartheta_i B_i^{d-1}(\xi)$;

    $\omega(\xi) \leftarrow \sum_{i=0}^{d_k} \omega_i B_i^{d_k}(\xi)$;

    par $\leftarrow \left\{\left\{\vartheta_0, \vartheta_1, \ldots, \vartheta_{d-1}\right\}, \left\{\omega_0, \omega_1, \ldots, \omega_{d_k}\right\}, \{\}\right\}$;

  else

    $\theta(\xi) \leftarrow \sum_{i=0}^{d} \vartheta_i B_i^d(\xi)$;

    $\ell \leftarrow \mathrm{argmax}\{\deg(\widetilde{\alpha}_j), j = 1, 2\}$;

    $\omega(\xi) \leftarrow \sum_{i=0}^{d_k+1} \omega_i B_i^{d_k+1}(\xi)$;

    $\omega_{d_k+1} \leftarrow$ solve $\mathrm{LeadCoef}(\omega) = -d\frac{\beta'_\ell(0)}{\mathrm{LeadCoef}(\widetilde{\alpha}_\ell)}\mathrm{LeadCoef}(\theta)$ for ω_{d_k+1};

    par $\leftarrow \left\{\left\{\vartheta_0, \vartheta_1, \ldots, \vartheta_d\right\}, \left\{\omega_0, \omega_1, \ldots, \omega_{d_k}\right\}, \{\}\right\}$;

  end

end

$r_\ell(\xi) \leftarrow \widetilde{\alpha}_\ell(\xi)\omega(\xi) + \beta_\ell(\xi)\theta'(\xi)$, $\ell = 1, 2$;

$\eta_\ell(\xi) \leftarrow \mathrm{quot}(r_\ell(\xi), \beta(\xi); \xi)$, $\ell = 1, 2$;

return $\left\{\theta(\xi), \omega(\xi), \eta_1(\xi), \eta_2(\xi), \mathbf{par}\right\}$

Output: trace function $\theta(\xi)$, scaled directional derivative $\omega(\xi)$, polynomials $\eta_1(\xi)$ and $\eta_2(\xi)$, free parameters **par**.

Algorithm 3: compute $\widehat{\tau}$ and $\widehat{\omega}$ (`TrAndDerRem`)

Input: polynomials $\widehat{\alpha}_1$, $\widehat{\alpha}_2$, $\widehat{\beta}_1$, $\widehat{\beta}_2$, β

% Case of linear non-uniformly parametrized edge

if $\beta(\xi) = \zeta^2(\xi)$ **then**

  return $\left\{\widehat{\tau}(\xi) \leftarrow \mu_1\zeta(\xi),\ \widehat{\omega}(\xi) \leftarrow 0, \left\{\mu_1, \emptyset\right\}\right\}$

end

% Parabolic edge, the generic case:

if $\widehat{\alpha}_1\widehat{\beta}_2 - \widehat{\alpha}_2\widehat{\beta}_1 \not\equiv 0$ **then**

  if $\widehat{\alpha}_1 \not\equiv 0$ **then**

    return $\left\{\widehat{\tau}(\xi) \leftarrow \mu_1\widehat{\alpha}_1(\xi) + \mu_2\widehat{\alpha}_2(\xi),\ \widehat{\omega}(\xi) \leftarrow -\mu_1\widehat{\beta}_1(\xi) - \mu_2\widehat{\beta}_2(\xi), \left\{\mu_1, \mu_2\right\}\right\}$

  else

    return $\left\{\widehat{\tau}(\xi) \leftarrow \mu_2\widehat{\alpha}_1(\xi) + \mu_1\widehat{\alpha}_2(\xi),\ \widehat{\omega}(\xi) \leftarrow -\mu_2\widehat{\beta}_1(\xi) - \mu_1\widehat{\beta}_2(\xi), \left\{\mu_1, \mu_2\right\}\right\}$

  end

end

% Parabolic edge, different special configurations when $\widehat{\alpha}_1\widehat{\beta}_2 \equiv \widehat{\alpha}_2\widehat{\beta}_1$:

if $\widehat{\beta}_1 \equiv 0$ and $\widehat{\beta}_2 \equiv 0$ **then**

  return $\left\{\widehat{\tau}(\xi) \leftarrow \mu_1\xi + \mu_2,\ \widehat{\omega}(\xi) \leftarrow 0, \left\{\mu_1, \mu_2\right\}\right\}$

end

if $\widehat{\alpha}_1 \equiv 0$ and $\widehat{\beta}_1 \equiv 0$ **then** $L = 2$ **else** $L = 1$ **end**;

$\zeta(\xi) \leftarrow \gcd(\widehat{\alpha}_1(\xi), \widehat{\alpha}_2(\xi), \widehat{\beta}_1(\xi), \widehat{\beta}_2(\xi); \xi)$;

if $\deg\zeta = 1$ or ($\deg\widehat{\alpha}_1 = 0$ and $\deg\widehat{\alpha}_2 = 0$ and $\deg\widehat{\beta}_1 = 0$ and $\deg\widehat{\beta}_2 = 0$) **then**

  return $\left\{\widehat{\tau}(\xi) \leftarrow \mathrm{LeadCoef}(\widehat{\alpha}_L)(\mu_1\xi + \mu_2),\ \widehat{\omega}(\xi) \leftarrow -\mathrm{LeadCoef}(\widehat{\beta}_L)(\mu_1\xi + \mu_2), \left\{\mu_1, \mu_2\right\}\right\}$

end

if $\widehat{\alpha}_1(\xi) = c\widehat{\beta}_1(\xi)$ and $\widehat{\alpha}_2(\xi) = c\widehat{\beta}_2(\xi)$ **then**

  return $\left\{\widehat{\tau}(\xi) \leftarrow c(\mu_1\xi + \mu_2),\ \widehat{\omega}(\xi) \leftarrow \mu_1\xi + \mu_2, \left\{\mu_1, \mu_2\right\}\right\}$

end

if $\deg\widehat{\alpha}_L = 1$ **then**

  compute b_0, b_1, c_0, c_1, c_2 so that $\widehat{\beta}_L(\xi) = b_0 + b_1\widehat{\alpha}_L(\xi)$, $\beta(\xi) = c_0 + c_1\widehat{\alpha}_L(\xi) + c_2\widehat{\alpha}_L^2(\xi)$;

  $\widehat{\tau}(\xi) \leftarrow \mu_1\widehat{\alpha}_L(\xi) + \mu_2$;

  $\widehat{\omega}(\xi) \leftarrow \frac{1}{c_0}\left(\mu_2 b_0 c_2 - \mu_1 b_1 c_0\right)\widehat{\alpha}_L(\xi) + \frac{\mu_2}{c_0}\left(b_0 c_1 - b_1 c_0\right) - \mu_1 b_0$;

else

  compute a_0, c_0, c_1, c_2 so that $\widehat{\alpha}_L(\xi) = a_0$, $\beta(\xi) = c_0 + c_1\widehat{\beta}_L(\xi) + c_2\widehat{\beta}_L^2(\xi)$;

  $\widehat{\tau}(\xi) \leftarrow \mu_2\frac{a_0 c_2}{c_0}\widehat{\beta}_L(\xi) + \mu_2\frac{a_0 c_1}{c_0} - \mu_1 a_0$;

  $\widehat{\omega}(\xi) \leftarrow \mu_1\widehat{\beta}_L(\xi) + \mu_2$;

end

return $\left\{\widehat{\tau}(\xi),\ \widehat{\omega}(\xi), \left\{\mu_1, \mu_2\right\}\right\}$;

Output: polynomials $\widehat{\tau}(\xi)$ and $\widehat{\omega}(\xi)$, free parameters $\left\{\mu_1, \mu_2\right\}$

Algorithm 4: `EdgePoints`

Input: $N^e_{k,1}$, $N^e_{k,2}$, $N^e_{k,3}$

$\boldsymbol{u} \leftarrow \left\{ \frac{j}{N^e_{k,2}+N^e_{k,3}+1}; j = 1, 2, \dots, N^e_{k,2} + N^e_{k,3} \right\}$;

$\text{ind} \leftarrow \left\lceil \frac{N^e_{k,2}+N^e_{k,3}}{2} \right\rceil$;

if $N^e_{k,3} = 1$ **then**

  $\left\{ \xi_{k,N^e_{k,2}+N^e_{k,3},1} \right\} \leftarrow \left\{ \boldsymbol{u}_{\text{ind}} \right\}$, $\left\{ \xi_{k,1,1}, \xi_{k,2,1}, \dots, \xi_{k,N^e_{k,2},1} \right\} \leftarrow \texttt{Drop}(\boldsymbol{u}, \text{ind})$;

else

  $\left\{ \xi_{k,N^e_{k,2}+N^e_{k,3},1} \right\} \leftarrow \{\}$, $\left\{ \xi_{k,1,1}, \xi_{k,2,1}, \dots, \xi_{k,N^e_{k,2},1} \right\} \leftarrow \boldsymbol{u}$;

end

if $N^e_{k,1} = N^e_{k,2}$ **then**

  $\left\{ \xi_{k,1,0}, \xi_{k,2,0}, \dots, \xi_{k,N^e_{k,1},0} \right\} \leftarrow \left\{ \xi_{k,1,1}, \xi_{k,2,1}, \dots, \xi_{k,N^e_{k,2},1} \right\}$;

else if $N^e_{k,1} = N^e_{k,2} - 1$ **then**

  $\left\{ \xi_{k,1,0}, \xi_{k,2,0}, \dots, \xi_{k,N^e_{k,1},0} \right\} \leftarrow \texttt{Drop}(\left\{ \xi_{k,1,1}, \xi_{k,2,1}, \dots, \xi_{k,N^e_{k,2},1} \right\}, \left\lceil \frac{N^e_{k,2}}{2} \right\rceil)$;

else

  $\left\{ \xi_{k,1,0}, \xi_{k,2,0}, \dots, \xi_{k,N^e_{k,1},0} \right\} \leftarrow \texttt{Drop}(\left\{ \xi_{k,1,1}, \xi_{k,2,1}, \dots, \xi_{k,N^e_{k,2},1} \right\}, \{\left\lceil \frac{N^e_{k,2}}{2} \right\rceil, \left\lceil \frac{N^e_{k,2}}{2} \right\rceil + 1\})$;

end

Output: $\left\{ \xi_{k,1,0}, \xi_{k,2,0}, \dots, \xi_{k,N^e_{k,1},0} \right\}$, $\left\{ \xi_{k,1,1}, \xi_{k,2,1}, \dots, \xi_{k,N^e_{k,2},1} \right\}$, $\left\{ \xi_{k,N^e_{k,2}+N^e_{k,3},1} \right\}$

References

[1] C. de Boor, A Practical Guide To Splines, Springer New York, 2001.
[2] M.J. Lai, L.L. Schumaker, Spline Functions on Triangulations, Cambridge University Press, 2007.
[3] R.W. Clough, J.L. Tocher, Finite element stiffness matrices for analysis of plates in bending, in: Conf. on Matrix Methods in Structural Mechanics, Wright–Patterson Air Force Base, Ohio, 1965, pp. 515–545.
[4] H. Speleers, A normalized basis for reduced Clough–Tocher splines, Comput. Aided Geom. Design 27 (2010) 700–712.
[5] J. Kosinka, T.J. Cashman, Watertight conversion of trimmed CAD surfaces to Clough–Tocher splines, Comput. Aided Geom. Design 37 (2015) 25–41.
[6] T. Lyche, J.L. Merrien, Simplex-splines on the Clough–Tocher element, Comput. Aided Geom. Design 65 (2018) 76–92.
[7] J. Grošelj, M. Knez, Generalized C^1 Clough–Tocher splines for CAGD and FEM, Comput. Methods Appl. Mech. Engrg. (2022) 395.
[8] P.G. Ciarlet, The Finite Element Method for Elliptic Problems, second ed., SIAM: Society for Industrial and Applied Mathematics, 2002.
[9] T.J.R. Hughes, J.A. Cottrell, Y. Bazilevs, Isogeometric analysis: CAD, finite elements, NURBS, exact geometry and mesh refinement, Comput. Methods Appl. Mech. Engrg. 194 (2005) 4135–4195.
[10] N. Jaxon, X. Qian, Isogeometric analysis on triangulations, Comput. Aided Des. 46 (2014) 45–57.
[11] S. Xia, X. Wang, X. Qian, Continuity and convergence in rational triangular Bézier spline based isogeometric analysis, Comput. Methods Appl. Mech. Engrg. 297 (2015) 292–324.
[12] S. Xia, X. Qian, Generating high-quality high-order parametrization for isogeometric analysis on triangulations, Comput. Methods Appl. Mech. Engrg. 338 (2018) 1–26.
[13] M.J.D. Powell, M.A. Sabin, Piecewise quadratic approximations on triangles, ACM Trans. Math. Software 3 (1977) 316–325.
[14] P. Dierckx, On calculating normalized Powell–Sabin B-splines, Comput. Aided Geom. Design 15 (1997) 61–78.
[15] H. Speleers, C. Manni, F. Pelosi, M.L. Sampoli, Isogeometric analysis with Powell–Sabin splines for advection-diffusion-reaction problems, Comput. Methods Appl. Mech. Engrg. 221–222 (2012) 132–148.
[16] H. Speleers, C. Manni, Optimizing domain parameterization in isogeometric analysis based on Powell–Sabin splines, J. Comput. Appl. Math. 289 (2015) 68–86.
[17] J. Grošelj, M. Kapl, M. Knez, T. Takacs, V. Vitrih, C^1-smooth isogeometric spline functions of general degree over planar mixed meshes: The case of two quadratic mesh elements, Appl. Math. Comput. 460 (2024).
[18] J. Grošelj, M. Kapl, M. Knez, T. Takacs, V. Vitrih, A super-smooth C^1 spline space over planar mixed triangle and quadrilateral meshes, Comput. Math. Appl. 80 (2020) 2623–2643.